ENGINEERING RESEARCH INSTITUTE
UNIVERSITY OF MICHIGAN
ANN ARBOR

Final Report

WIND-TUNNEL TESTS ON OPEN-SIDED BUILDING MODELS

E. J. LESHER

Project 2295

SANDIA CORPORATION
CONTRACT NO. AEC AT(29-1)-789
ALBUQUERQUE, NEW MEXICO

February, 1955

SUMMARY

Tests of pressure distributions on both upper and lower surfaces of roofs of models of open-sided buildings were made in the University of Michigan low-speed wind tunnel. Results are presented in terms of nondimensional coefficients, tabulated and plotted.

ACKNOWLEDGMENT

The project was initiated through Rackham Research Grant R-277 in the Civil Engineering Department of the University.

WIND TUNNEL

The University of Michigan low-speed wind tunnel is of the double-return closed-throat type. The test-section cross section is shown in Fig. 1.

GROUND BOARD

During the tests a ground board was used, as shown in Figs. 1, 2, 4, and 5. The ground board was made of 3/4" plywood supported on longitudinal 2 x 4's. The leading edge of the ground board was rounded.

MODELS

Dimensions of the models used are shown in Fig. 3. Three models were constructed, for ϕ = 20, 25, and 30°. The material used was 3/8" fir plywood.

The pressure orifices were provided by means of Jessall pressure tape. This tape is 1" wide and about 1/16" thick and has twenty tubes. The tape was cemented to the model, and taken through the ground board as shown in Fig. 5. Below the test section, connections were made to a 40-tube inclined manometer. Orifices were punched into the tubes of the tape.

Figures 6 and 7 give the tape positions. The "end" tapes were placed as far to the left as possible, looking upstream. The center lines of the "quarter point" and "center" tapes were located at the quarter point and center of the 15" internal dimension of the model.

The axes of the orifice locations sloped as shown in Figs. 6 and 7. The tape-tube spacing is approximately 0.045". This information permits more precise lateral locations of orifices, if desired.

The roof faces are referred to as "front", "rear", "upper", and "lower", as shown in Figs. 6 and 7. Longitudinal orifice positions are given in terms of x = a/b, the nondimensional distance from the upstream edge of a roof face, as shown in Fig. 6.

VELOCITY DISTRIBUTION

The velocity distribution at a section 3 feet downstream from the upstream edge of the ground board was measured without model by means of a pitot static tube. The results are given in Fig. 8. Here, V is the air velocity; V_o is the value of V for the contour marked $V/V_o = 1.000$.

BOUNDARY-LAYER SURVEY

Boundary-layer measurements were made at three positions on the center line of the ground board without model, by means of a total head tube. The results are given in Fig. 9. Here, V is the air velocity; V_o is the velocity just ouside the boundary layer.

REGULATION OF TUNNEL SPEED

The factor relating dynamic pressure at the model position and pressure difference at two static orifices in the contraction cone was obtained with no model in the tunnel. The pressure difference at the static orifices was then used as the measure of tunnel speed during the pressure tests.

PRESSURE TESTS AND RESULTS

Pressure tests were made for ϕ = 20, 25, and 30°, with orifices at end, quarter point, center, upper, and lower.

Tests were made one spanwise station at a time; end, quarter point, or center. Only the two pressure tapes in use, upper and lower, were present on the model. The other four tapes were removed, thus keeping tape-interference effects at a minimum.

The tests were run at dynamic pressure, q = 3 cm, H_2O = 6.13 lb/ft^2, corresponding to velocity V = 71.9 ft/sec under standard sea-level conditions. The average temperature during tests was 76°F, and average pressure was 29.0 in Hg, corresponding to relative density σ = 0.938. Actual test velocities hence averaged 74.3 ft/sec.

The results of the tests are given in Tables 1 through 11 and in Figs. 10 through 28. Tables 1 through 9 and Figs. 10 through 27 present pressures in terms of the pressure coefficient P, where the following definitions are used:

$$P = \frac{p-p_o}{q} ,$$

p = static pressure at orifice,
p_o = static pressure of uniform stream,
q = $1/2\ \rho\ V_o^2$ = dynamic pressure of uniform stream,
ρ = mass density of air, and
V_o = velocity of uniform stream.

The areas between the curves of Figs. 10 through 27 were measured, giving values of the section normal force coefficient,

$$c_n = \frac{\text{normal force/unit span}}{\text{roof width parallel to surface x } q} .$$

The results are tabulated in Table 10 and plotted in Fig. 28. In this figure,

$$y = \frac{\text{distance from end of roof}}{\text{span of roof}} .$$

The areas under the curves of Fig. 28 were measured, giving values of

$$C_N = \frac{\text{normal force on roof}}{\text{area of roof x } q}$$

Values of lift and drag coefficient were calculated, where

$$C_L = \frac{\text{lift on roof}}{\text{projected area of roof in top view x } q}$$

$$C_D = \frac{\text{drag on roof}}{\text{projected area of roof in top view x } q}$$

$$C_L = C_N$$

$$C_D = -C_N \tan \phi \text{ (front roof)}$$

$$C_D = C_N \tan \phi \text{ (rear roof)}$$

The lift is the aerodynamic force perpendicular to the wind, while drag is the force parallel to the wind.

Note that these force coefficients are based on the area of a particular roof, front or rear, and not on total roof area.

For civil engineering purposes a drag coefficient based on projected area of roof in front view may be desired. This is defined as

$$C_F = \frac{\text{total drag of front and rear roofs}}{\text{projected area in front view x q}}$$

$$= C_{N_{\text{front roof}}} + C_{N_{\text{rear roof}}} .$$

Values of C_N, C_L, C_D, and C_F are tabulated in Table 11.

It should be noted that all forces presented are due to normal pressure and do not include skin-friction forces.

TESTS WITH BRASS-PLATE ORIFICES

Some tests were made with models which had the pressure orifices in inset brass plates. The results agreed well with results using pressure tape. However, this method was not very satisfactory for the following reasons:

1. Orifices were not provided close to eaves and ridge of roof.

2. The copper tubing to orifice plates could not be well faired into the roof.

3. Plugged orifices caused trouble.

These models were discarded and new models constructed for use with the pressure tape.

TABLE 1. PRESSURES

$\phi = 20°$

Orifices at End

Upper			Lower		
Orifice	x	P	Orifice	x	P
		Front			
1	.033	.129	21	.033	-.245
2	.084	.180	22	.094	-.249
3	.201	.103	23	.202	-.283
4	.318	.056	24	.317	-.279
5	.434	.017	25	.424	-.279
6	.553	-.017	26	.551	-.283
7	.672	-.056	27	.679	-.232
8	.791	-.103	28	.794	-.069
9	.893	-.146	29	.901	-.197
10	.967	-.283	30	.963	-.124
		Rear			
11	.020	-.335	31	.033	-.107
12	.092	-.355	32	.090	-.120
13	.200	-.339	33	.197	-.021
14	.318	-.322	34	.311	.120
15	.441	-.382	35	.439	.202
16	.555	-.403	36	.553	-.167
17	.676	-.421	37	.676	-.193
18	.790	-.433	38	.791	-.288
19	.896	-.451	39	.893	.000
20	.961	-.403	40	.963	-.249

TABLE 2. PRESSURES

$\phi = 20°$

Orifices at Quarter Point

Upper			Lower		
Orifice	x	P	Orifice	x	P
		Front			
1	.033	.481	21	.033	-.373
2	.084	.416	22	.099	-.365
3	.201	.313	23	.206	-.339
4	.320	.223	24	.317	-.339
5	.434	.172	25	.440	-.343
6	.553	.112	26	.556	-.352
7	.672	.030	27	.679	-.249
8	.791	-.043	28	.794	-.249
9	.896	-.146	29	.901	-.185
10	.969	-.361	30	.963	-.219
		Rear			
11	.020	-.395	31	.039	-.155
12	.090	-.382	32	.098	-.210
13	.201	-.365	33	.197	-.107
14	.320	-.378	34	.320	.026
15	.443	-.416	35	.443	.180
16	.553	-.446	36	.557	.253
17	.676	-.464	37	.676	.249
18	.791	-.464	38	.791	.172
19	.902	-.536	39	.895	.043
20	.963	-.519	40	.963	-.172

TABLE 3. PRESSURES

$\phi = 20°$

Orifices at Center

Upper			Lower		
Orifice	x	P	Orifice	x	P
		Front			
1	.033	.511	21	.030	-.215
2	.082	.446	22	.095	-.223
3	.203	.330	23	.203	-.245
4	.321	.232	24	.317	-.249
5	.438	.145	25	.441	-.262
6	.557	.103	26	.555	-.300
7	.677	.060	27	.688	-.300
8	.798	-.021	28	.796	-.266
9	.903	-.116	29	.905	-.266
10	.977	-.258	30	.966	-.197
		Rear			
11	.026	-.305	31	.039	-.232
12	.097	-.305	32	.099	-.258
13	.206	-.313	33	.202	-.223
14	.326	-.343	34	.322	-.133
15	.450	-.361	35	.448	-.039
16	.565	-.386	36	.561	.060
17	.689	-.403	37	.684	.094
18	.804	-.412	38	.799	.086
19	.913	-.378	39	.904	.009
20	.977	-.356	40	.972	-.146

TABLE 4. PRESSURES

$\phi = 25°$

Orifices at End

Upper			Lower		
Orifice	x	P	Orifice	x	P
		Front			
1	.028	.442	21	.028	-.425
2	.081	.352	22	.075	-.403
3	.177	.232	23	.178	-.442
4	.308	.133	24	.304	-.476
5	.435	.086	25	.431	-.485
6	.561	.026	26	.555	-.498
7	.684	-.004	27	.684	-.524
8	.818	-.047	28	.816	-.545
9	.913	-.094	29	.913	-.459
10	.972	-.309	30	.968	-.356
		Rear			
11	.026	-.335	31	.024	-.386
12	.081	-.330	32	.075	-.459
13	.181	-.335	33	.170	-.399
14	.308	-.361	34	.300	-.318
15	.435	-.378	35	.427	-.112
16	.559	-.403	36	.553	.090
17	.686	-.429	37	.680	.193
18	.818	-.455	38	.810	.172
19	.917	-.476	39	.905	.[illegible]
20	.972	-.494	40	.966	-.236

TABLE 5. PRESSURES

$\phi = 25°$

Orifices at Quarter Point

Upper			Lower		
Orifice	x	P	Orifice	x	P
		Front			
1	.026	.742	21	.032	-.468
2	.079	.605	22	.079	-.476
3	.175	.494	23	.183	-.472
4	.306	.365	24	.306	-.485
5	.433	.279	25	.433	-.511
6	.560	.210	26	.560	-.541
7	.683	.124	27	.687	-.614
8	.813	.021	28	.821	-.567
9	.913	-.086	29	.917	-.429
10	.972	-.206	30	.974	-.416
		Rear			
11	.022	-.348	31	.026	-.429
12	.075	-.292	32	.079	-.511
13	.175	-.361	33	.171	-.519
14	.306	-.378	34	.306	-.425
15	.429	-.403	35	.433	-.249
16	.556	-.429	36	.556	-.039
17	.683	-.442	37	.683	.116
18	.813	-.433	38	.813	.142
19	.913	-.433	39	.909	.056
20	.968	-.442	40	.968	-.142

TABLE 6. PRESSURES

$\phi = 25°$

Orifices at Center

Upper			Lower		
Orifice	x	P	Orifice	x	P
		Front			
1	.027	.730	21	.026	-.365
2	.080	.601	22	.076	-.365
3	.176	.481	23	.175	-.373
4	.309	.369	24	.304	-.399
5	.434	.309	25	.433	-.425
6	.561	.215	26	.558	-.433
7	.685	.137	27	.687	-.498
8	.818	.026	28	.821	-.365
9	.917	-.082	29	.921	-.438
10	.975	-.253	30	.976	-.356
		Rear			
11	.032	-.300	31	.028	-.412
12	.084	-.305	32	.081	-.446
13	.185	-.322	33	.177	-.485
14	.313	-.339	34	.308	-.442
15	.438	-.373	35	.437	-.399
16	.564	-.386	36	.563	-.258
17	.690	-.395	37	.690	.030
18	.822	-.300	38	.820	-.043
19	.921	-.369	39	.918	-.064
20	.977	-.318	40	.978	-.206

TABLE 7. PRESSURES

$\phi = 30°$

Orifices at End

Upper			Lower		
Orifice	x	P	Orifice	x	P
		Front			
1	.027	.597	21	.026	-.519
2	.079	.412	22	.083	-.511
3	.171	.279	23	.166	-.528
4	.299	.163	24	.302	-.588
5	.432	.120	25	.430	-.597
6	.562	.056	26	.562	-.644
7	.695	.021	27	.698	-.708
8	.816	-.021	28	.826	-.648
9	.915	-.082	29	.917	-.515
10	.974	-.180	30	.966	-.433
		Rear			
11	.026	-.326	31	.026	-.464
12	.079	-.318	32	.060	-.541
13	.169	-.330	33	.166	-.588
14	.301	-.348	34	.298	-.528
15	.440	-.365	35	.426	-.330
16	.568	-.382	36	.562	-.021
17	.699	-.412	37	.690	.197
18	.827	-.425	38	.823	.253
19	.929	-.416	39	.921	.086
20	.977	-.472	40	.966	-.099

TABLE 8. PRESSURES

$\phi = 30°$

Orifices at Quarter Point

Upper			Lower		
Orifice	x	P	Orifice	x	P
		Front			
1	.028	.884	21	.030	-.584
2	.079	.738	22	.085	-.614
3	.170	.584	23	.162	-.614
4	.298	.476	24	.302	-.609
5	.434	.382	25	.426	-.614
6	.562	.279	26	.566	-.691
7	.698	.197	27	.702	-.734
8	.819	.094	28	.826	-.695
9	.917	-.039	29	.917	-.579
10	.975	-.215	30	.966	-.515
		Rear			
11	.024	-.330	31	.030	-.554
12	.075	-.335	32	.064	-.554
13	.166	-.348	33	.170	-.665
14	.302	-.378	34	.302	-.601
15	.438	-.399	35	.427	-.506
16	.566	-.395	36	.563	-.296
17	.698	-.459	37	.692	-.039
18	.826	-.468	38	.820	.094
19	.928	-.472	39	.919	.073
20	.977	-.481	40	.964	-.172

TABLE 9. PRESSURES

$\phi = 30°$

Orifices at Center

Upper			Lower		
Orifice	x	P	Orifice	x	P
		Front			
1	.020	.803	21	.028	-.437
2	.102	.622	22	.104	-.450
3	.205	.515	23	.215	-.416
4	.329	.429	24	.334	-.455
5	.446	.343	25	.452	-.515
6	.567	.266	26	.573	-.562
7	.692	.189	27	.696	-.567
8	.810	.107	28	.822	-.545
9	.910	-.034	29	.917	-.309
10	.978	-.021	30	.977	-.399
		Rear			
11	.026	-.026	31	.030	-.437
12	.089	-.197	32	.094	-.511
13	.185	-.292	33	.189	-.592
14	.306	-.309	34	.312	-.601
15	.425	-.335	35	.432	-.571
16	.546	-.352	36	.556	-.459
17	.667	-.343	37	.673	-.322
18	.788	-.339	38	.790	-.185
19	.896	-.300	39	.893	-.099
20	.981	-.283	40	.972	-.176

TABLE 10

VALUES OF c_n

ϕ, degrees	End	Quarter Point	Center
	Front		
20	-.215	-.425	-.402
25	-.553	-.750	-.670
30	-.720	-.950	-.783
	Rear		
20	.335	.480	.265
25	.290	.200	.080
30	.200	.095	-.110

TABLE 11

FORCE COEFFICIENTS

ϕ, degrees	Front		Rear		Whole		
	C_N, C_L	C_D	C_N, C_L	C_D	C_L	C_D	C_F
20	-.38	.138	.41	.149	.015	.144	.79
25	-.70	.326	.20	.093	-.25	.220	.90
30	-.86	.496	.08	.046	-.39	.271	.94

Fig. 1. Tunnel Cross Section.

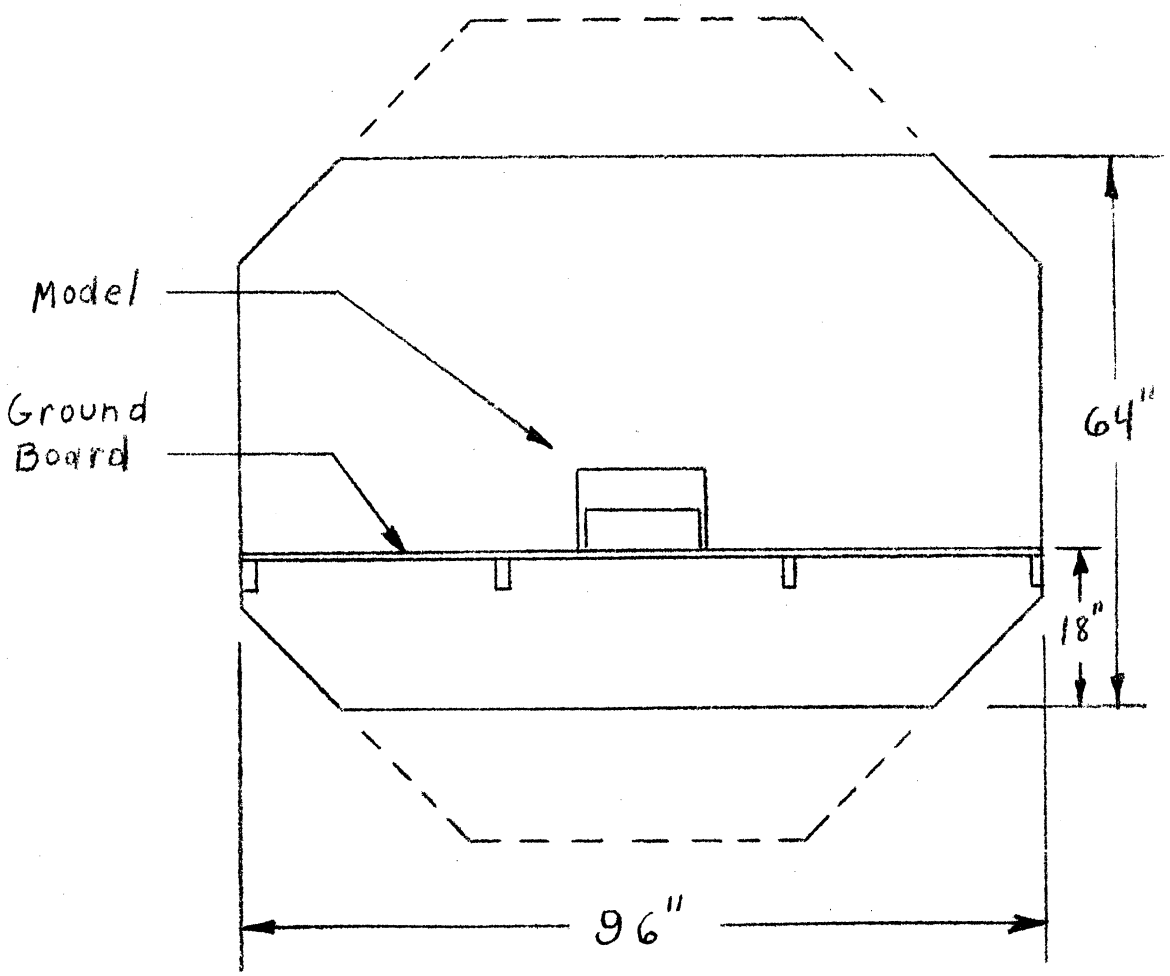

Fig. 2. Section through Test Section.

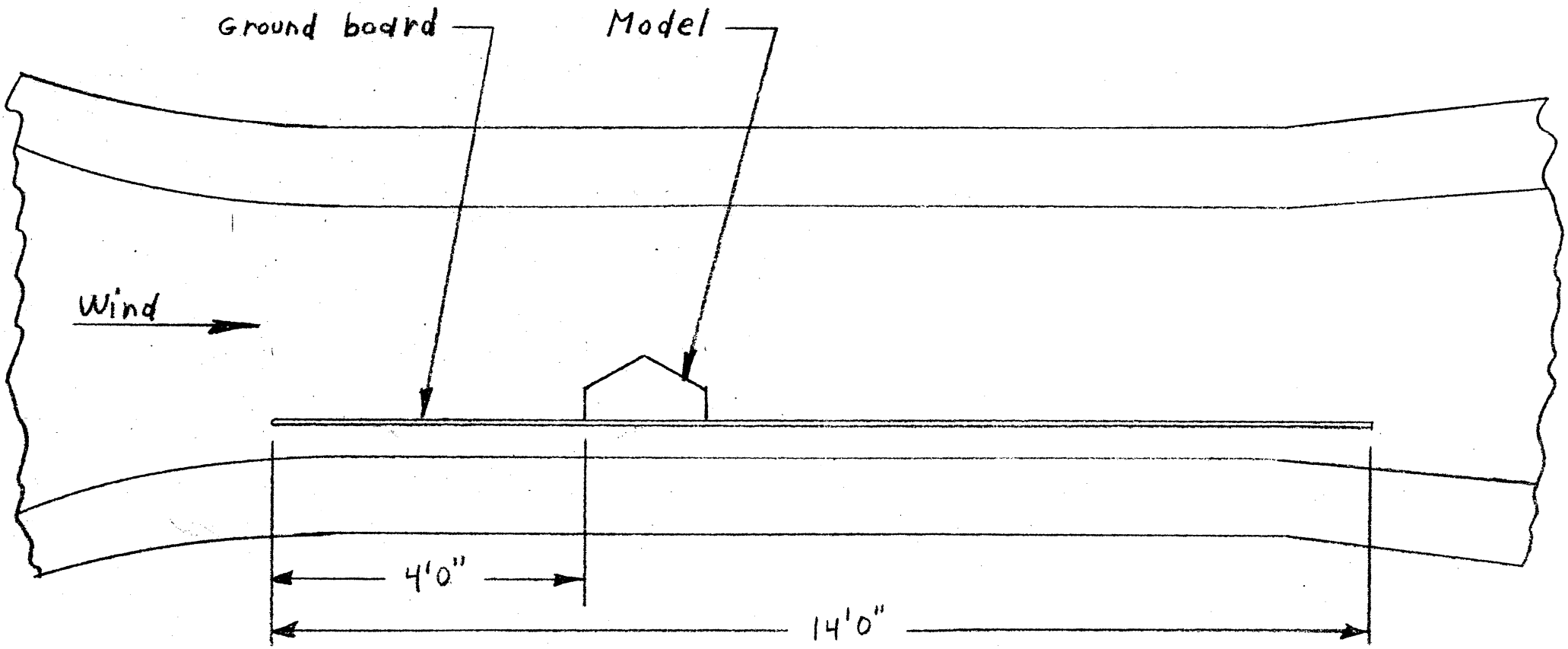

Fig. 3. Models.

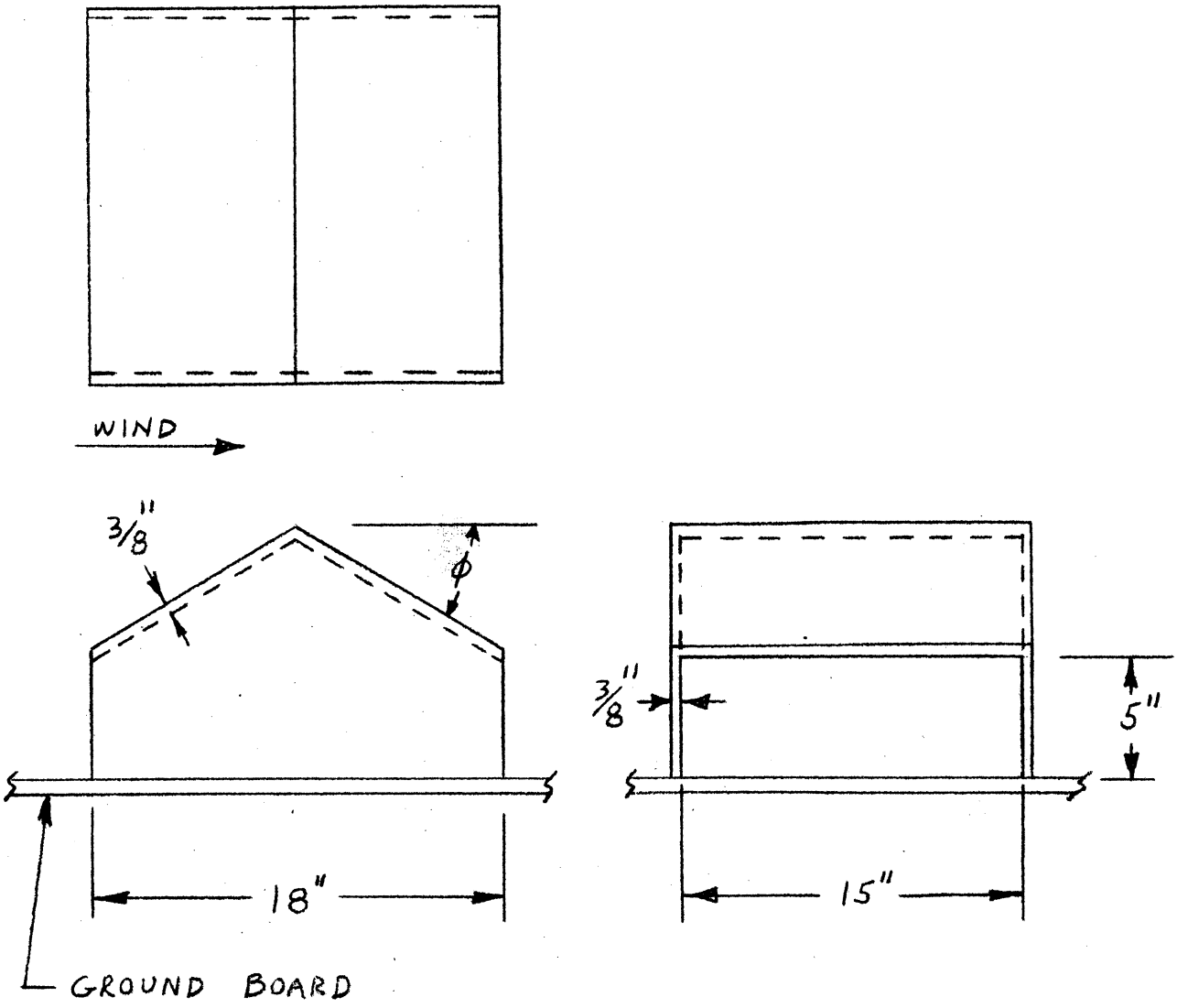

ϕ = 20°, 25°, and 30°

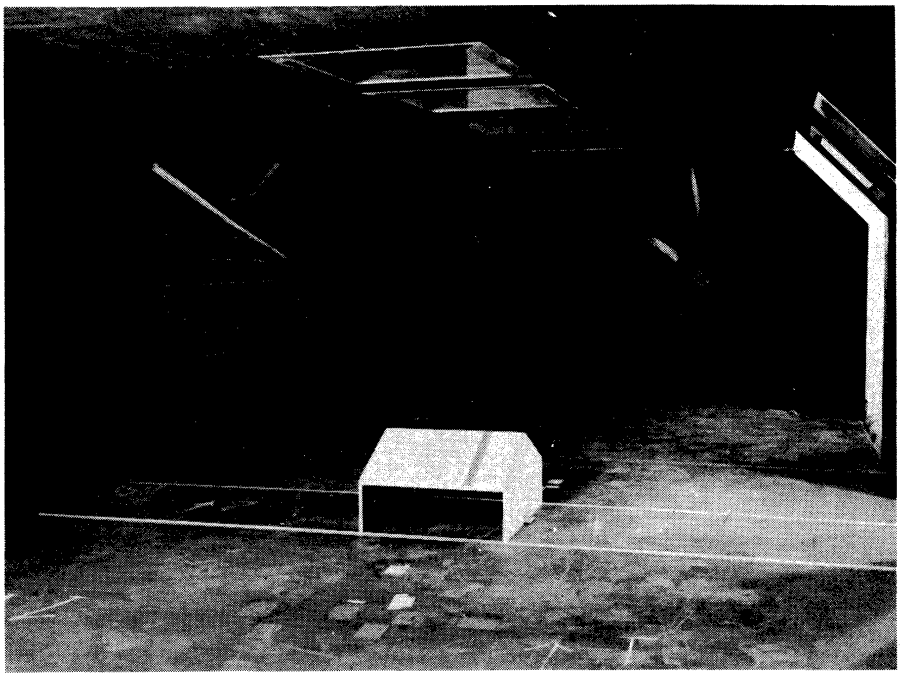

Fig. 4. Model in Wind Tunnel, Downstream View.

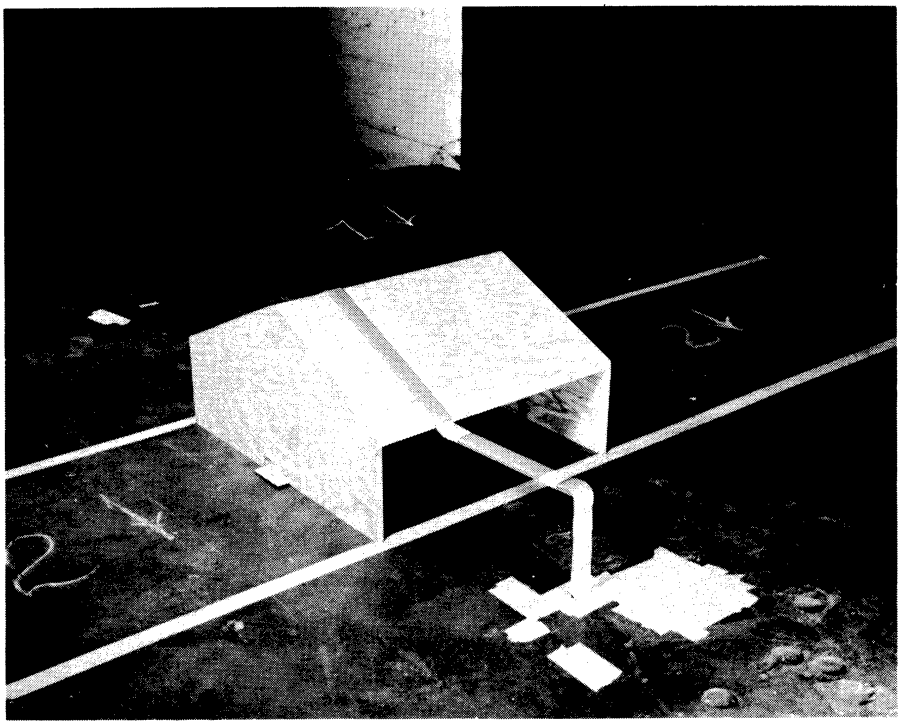

Fig. 5. Model in Wind Tunnel, Orifices at Quarter Point.

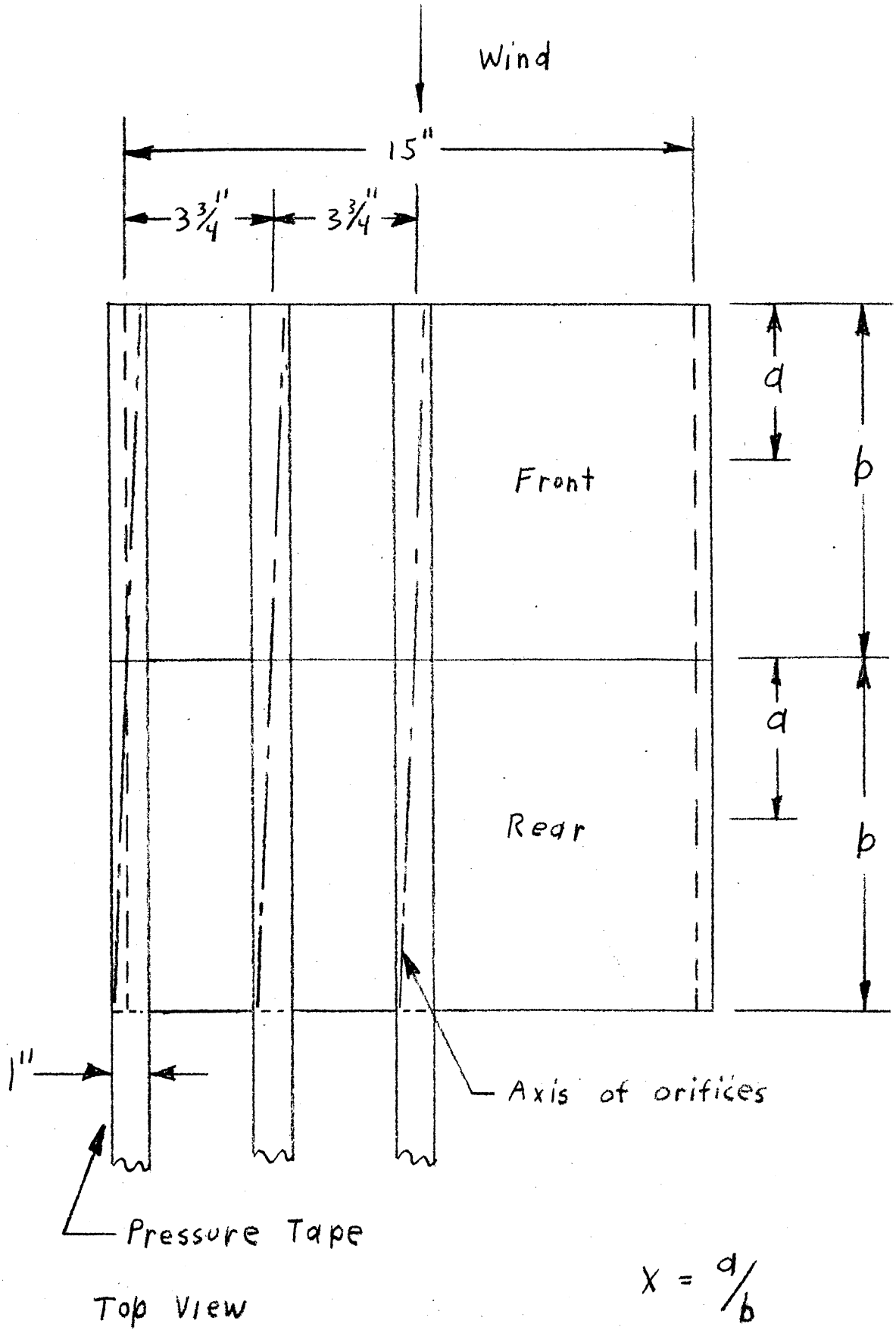

Fig. 6. Orifice Locations, Upper.

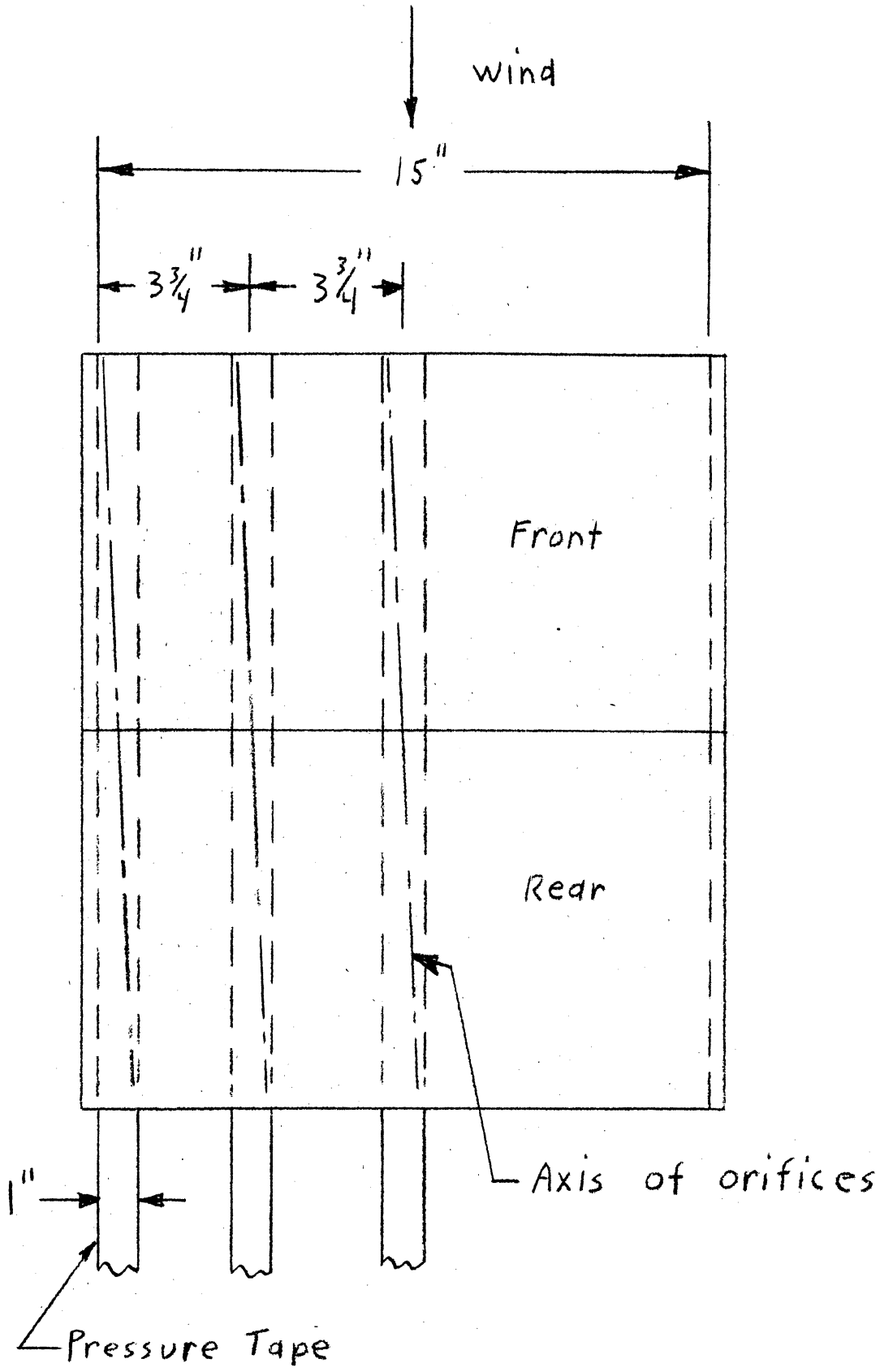

Fig. 7. Orifice Locations, Lower.

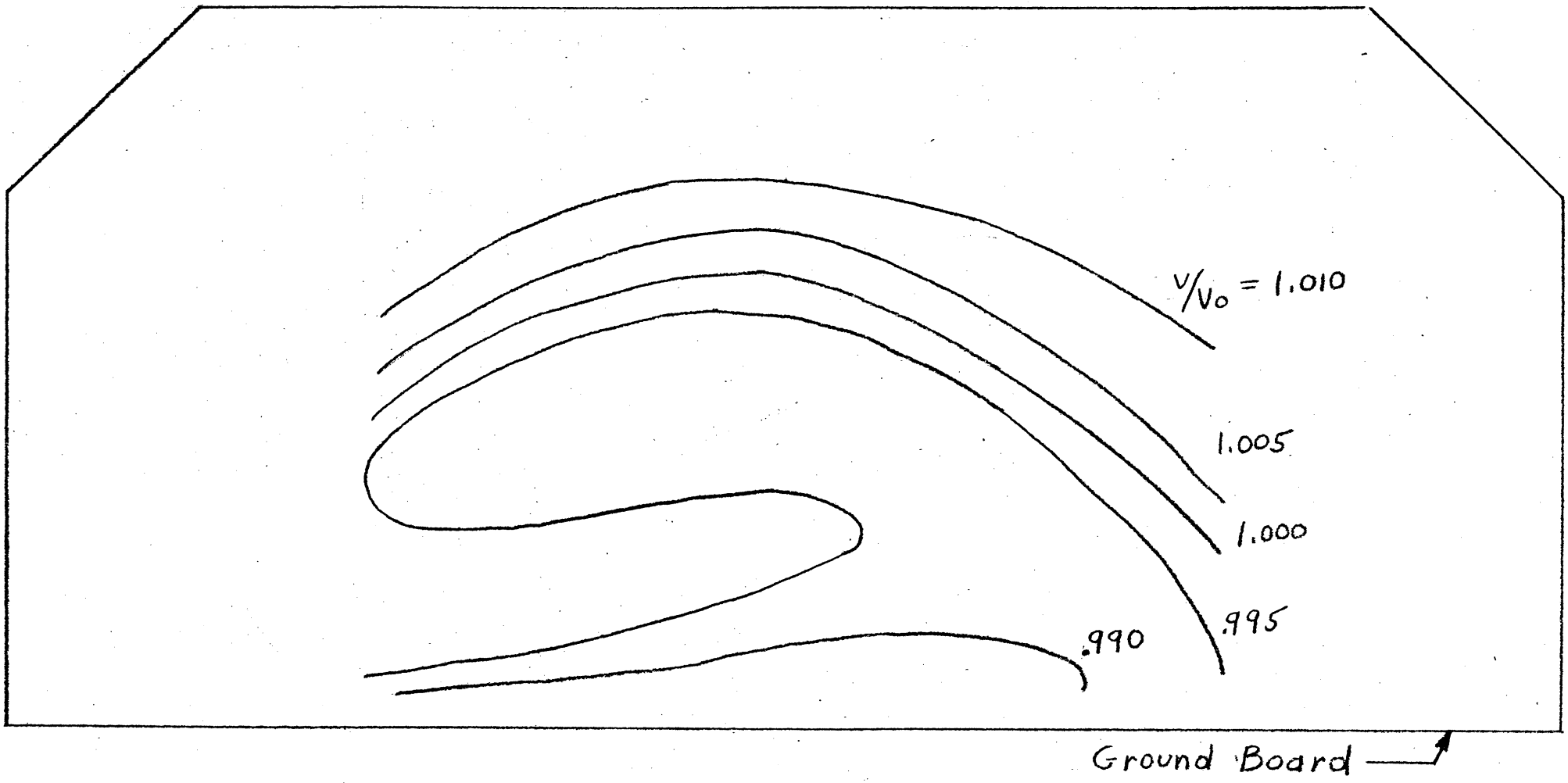

Fig. 8. Velocity Distribution at Model Location,
View Looking Upstream. Scale 1"=10"

Fig. 9. Velocity Distribution, Ground Board Boundary Layer.

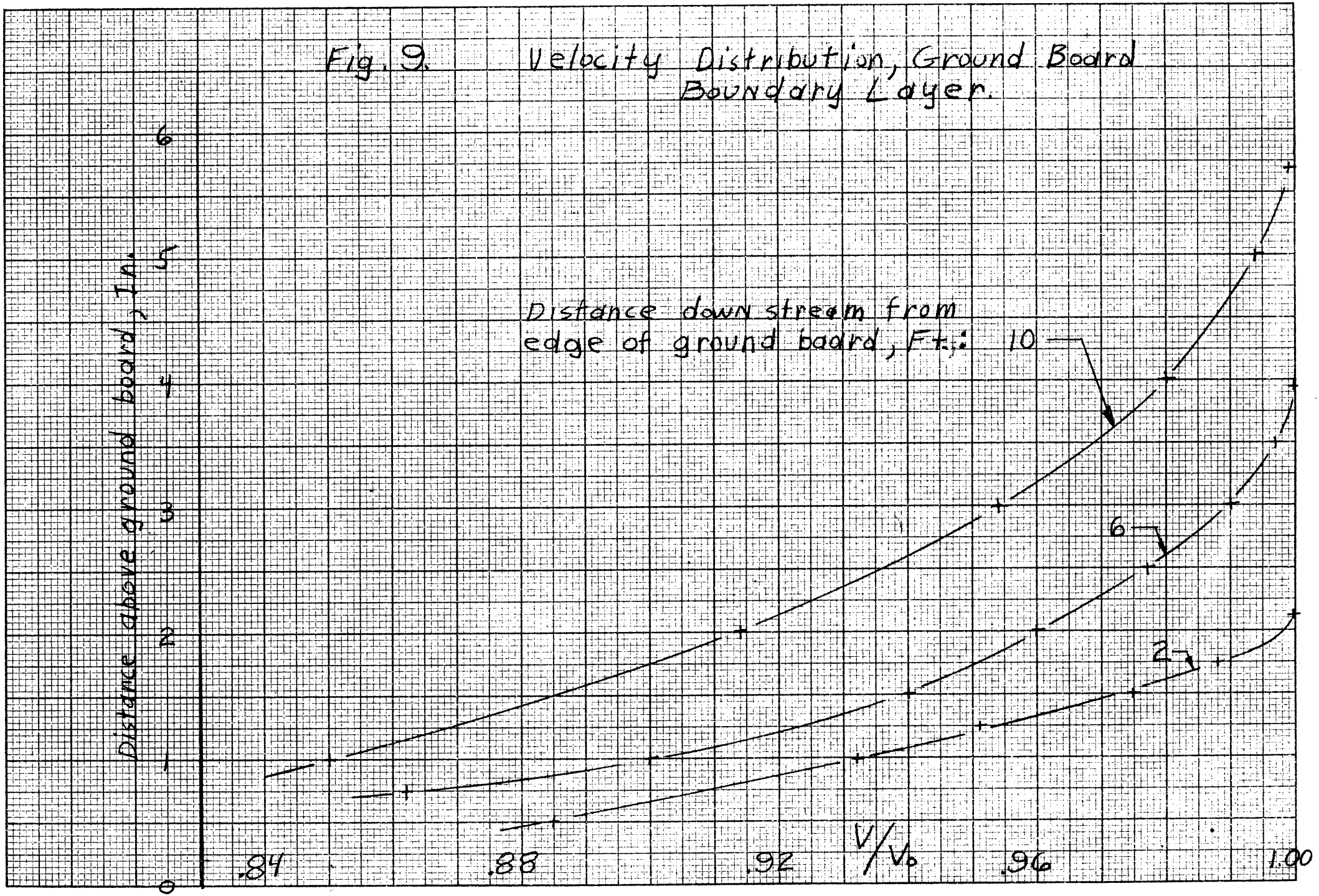

Fig. 10. P vs. X

Front, $\phi = 20°$

Orifices at end.

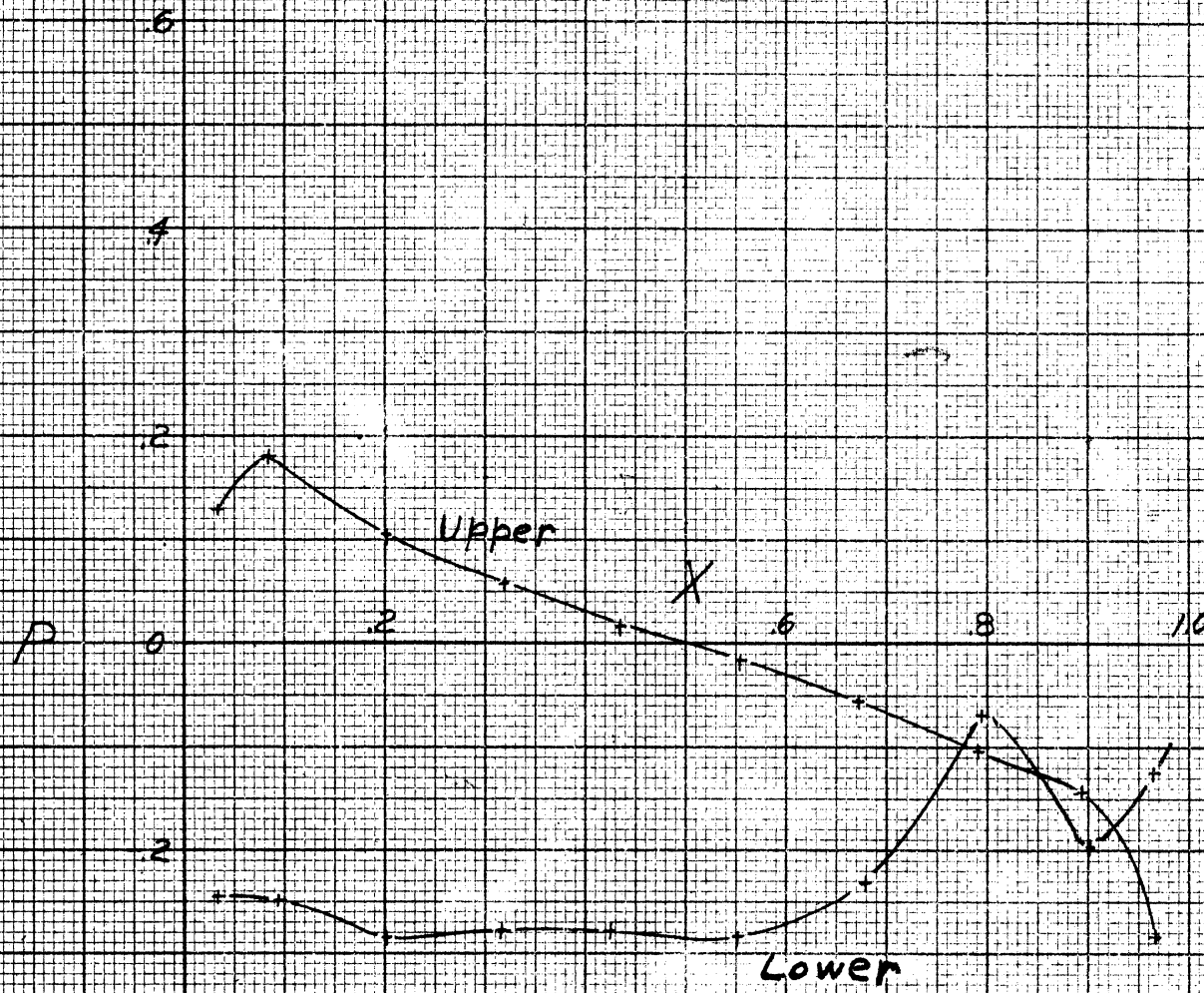

Fig. 11. P vs. X

Rear, $\phi = 20°$

Orifices at end.

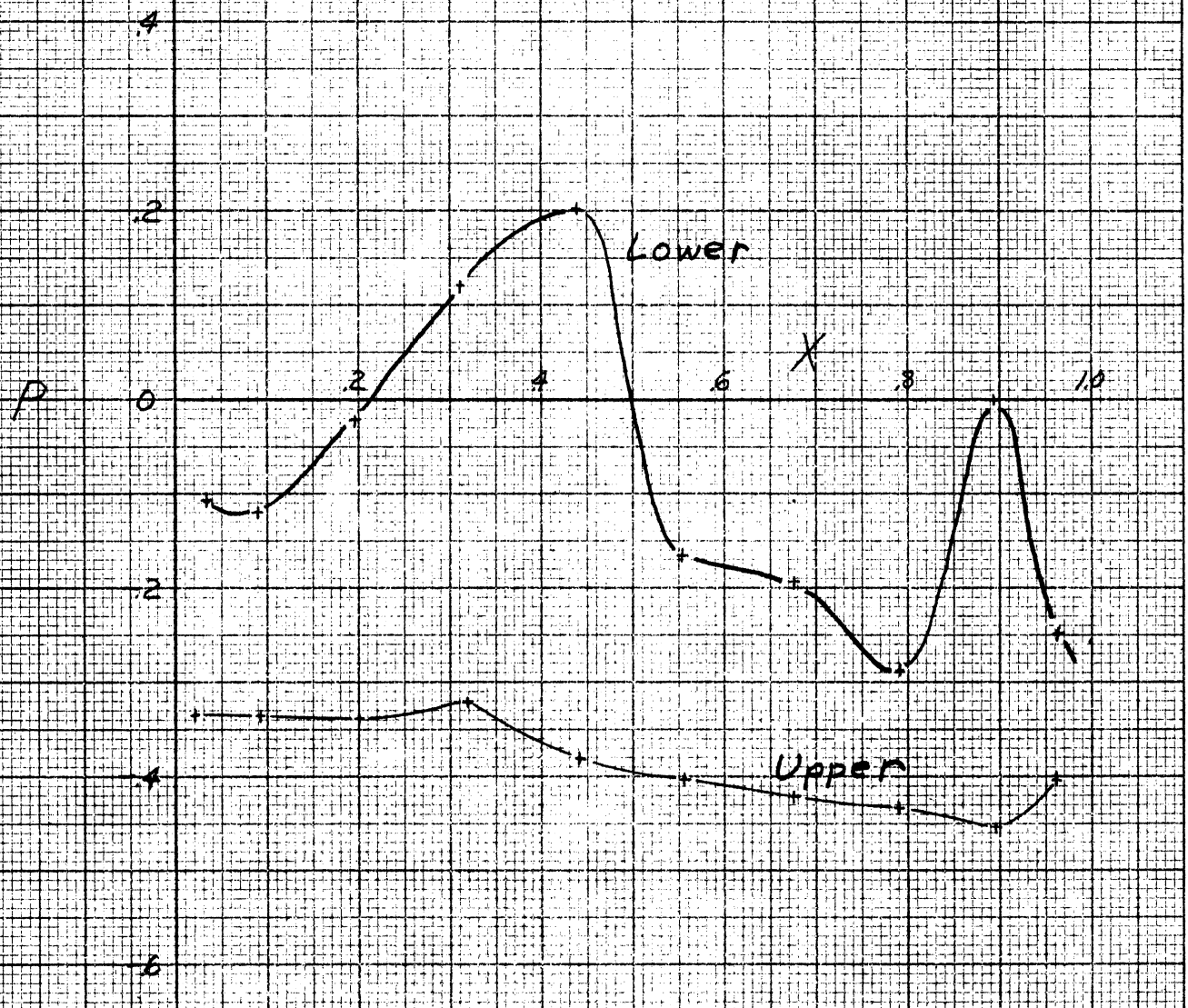

Fig. 12. P vs. X

Front, $\phi = 20°$

Orifices at quarter point.

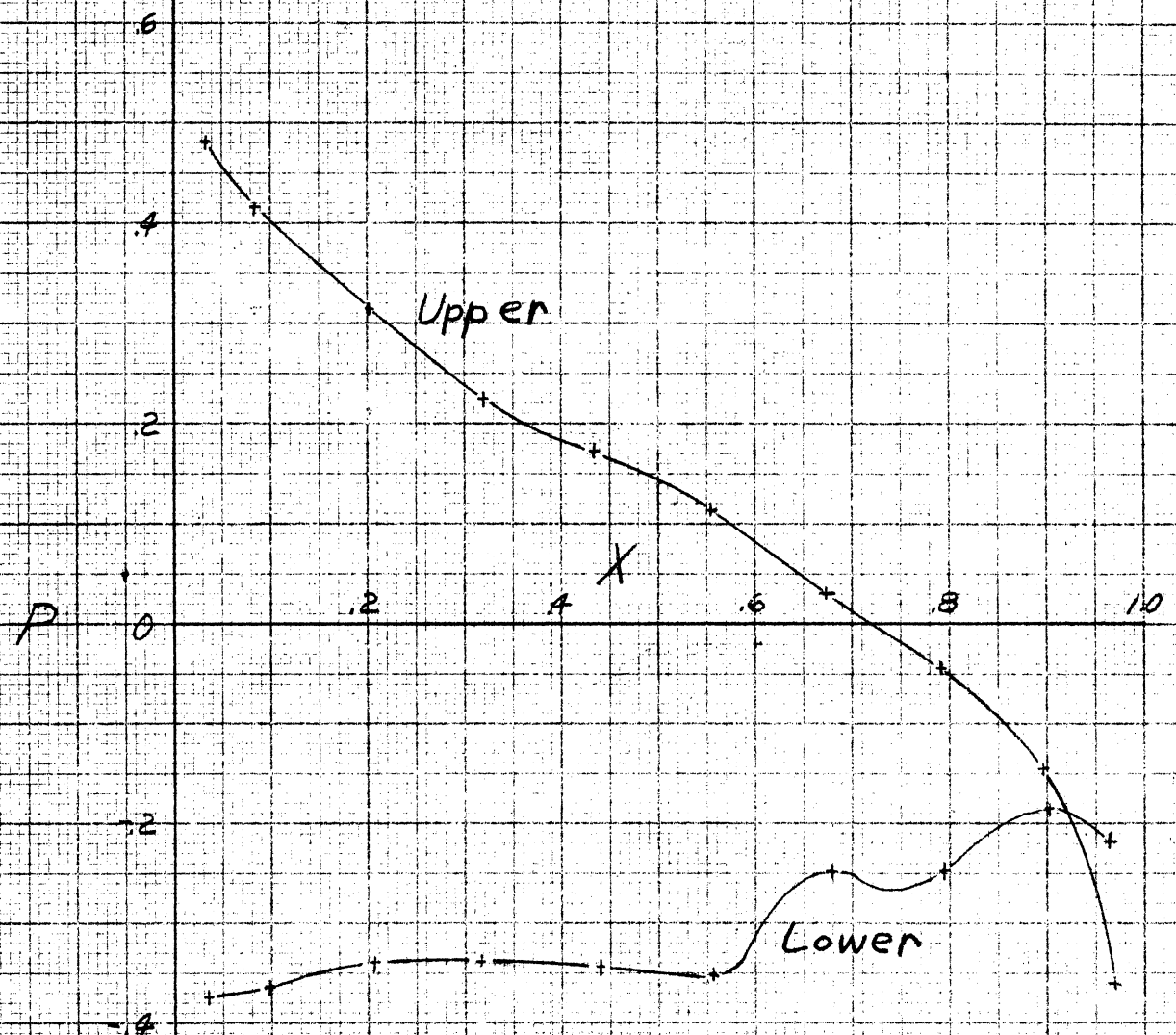

Fig. 13. P vs. X

Rear, $\phi = 20°$

Orifices at quarter point.

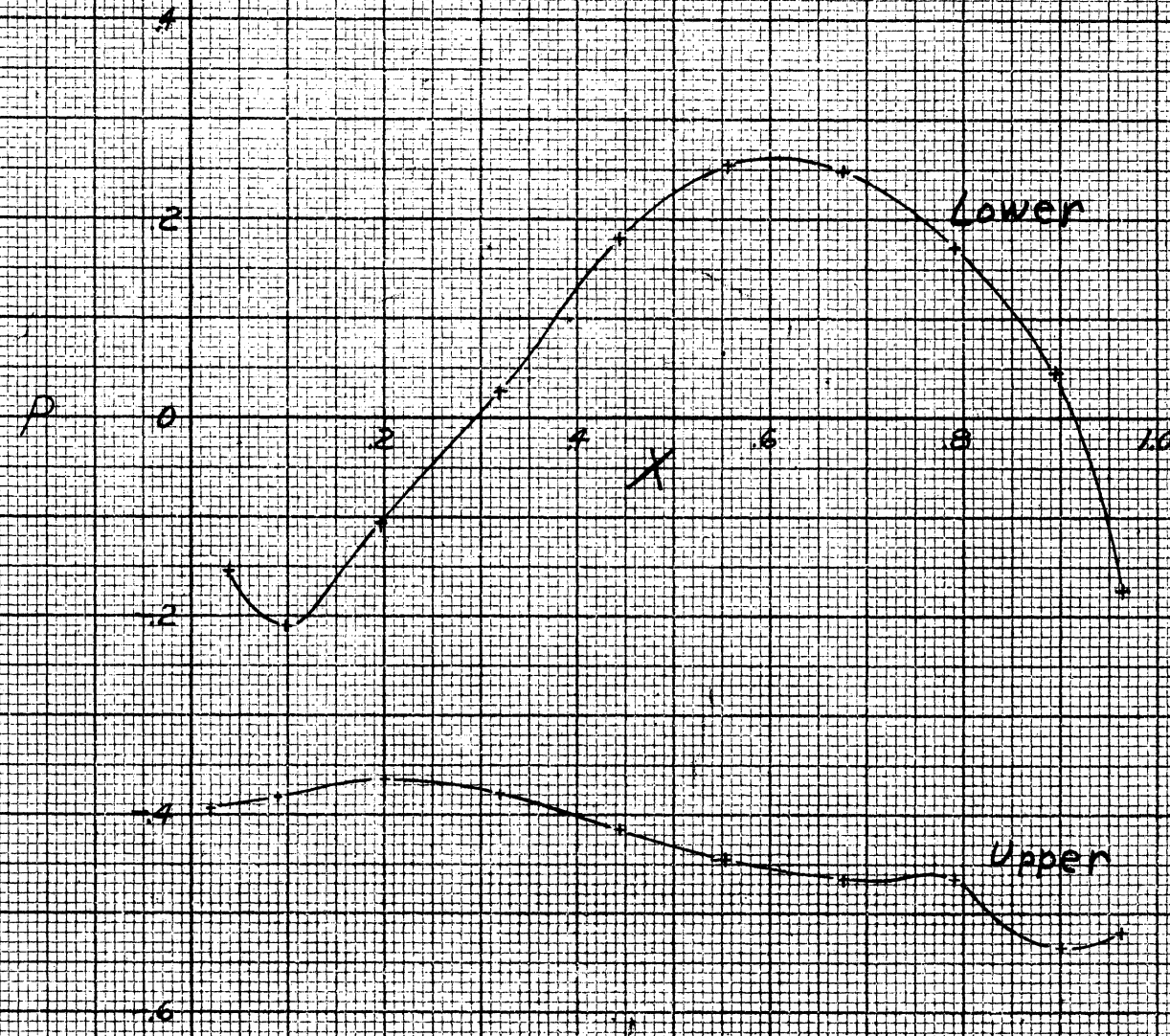

Fig. 14. P vs. X

Front, $\phi = 20^\circ$

Orifices at center.

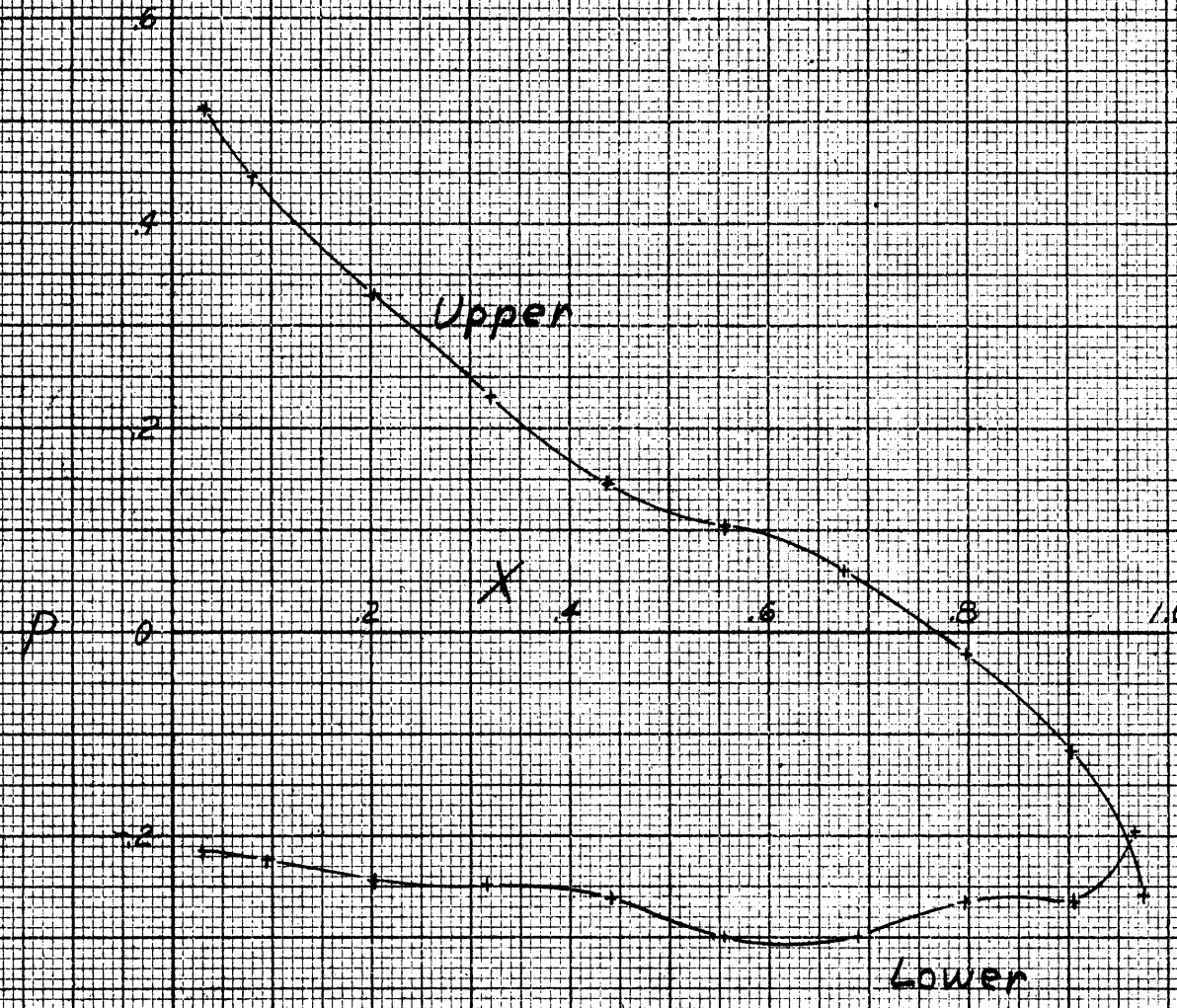

Fig. 15. P vs. X

Rear, $\phi = 20°$

Orifices at center.

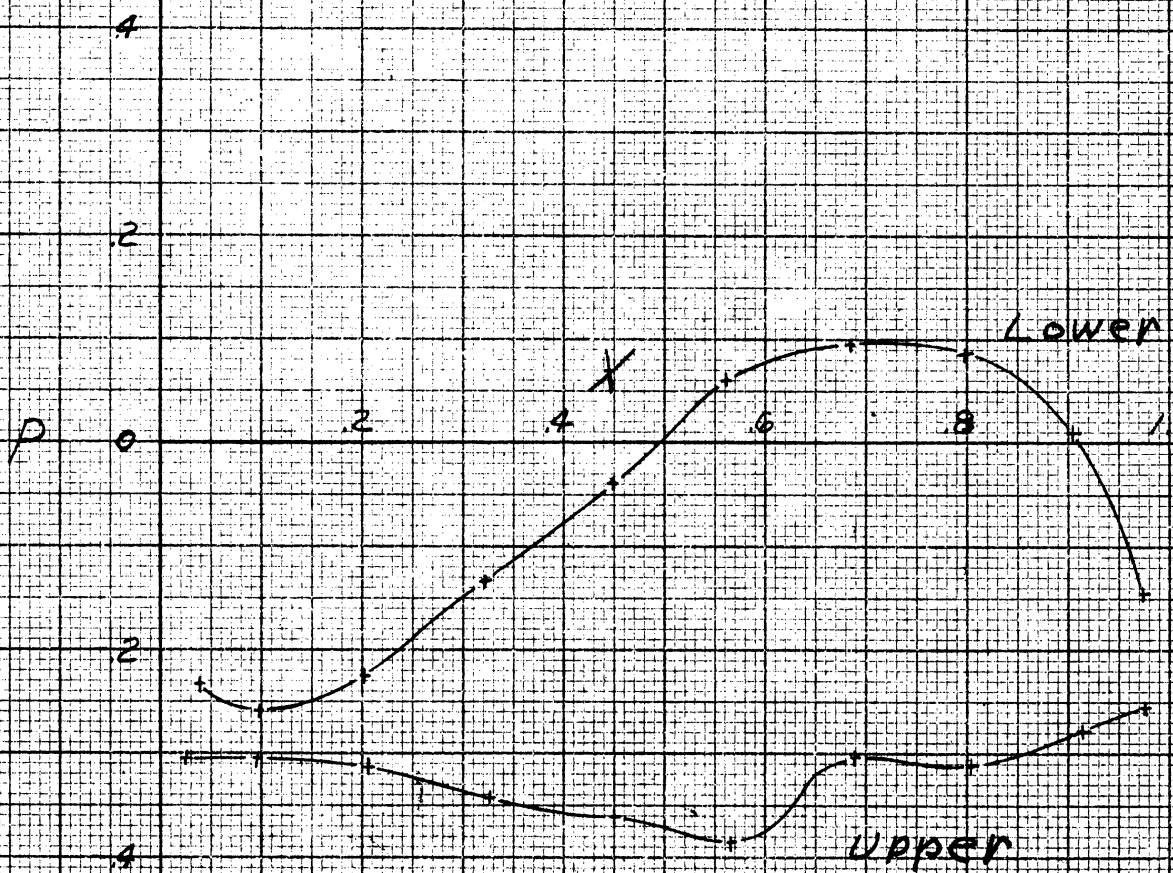

Fig. 16. P vs. X

Front, $\phi = 25°$

Orifices at end.

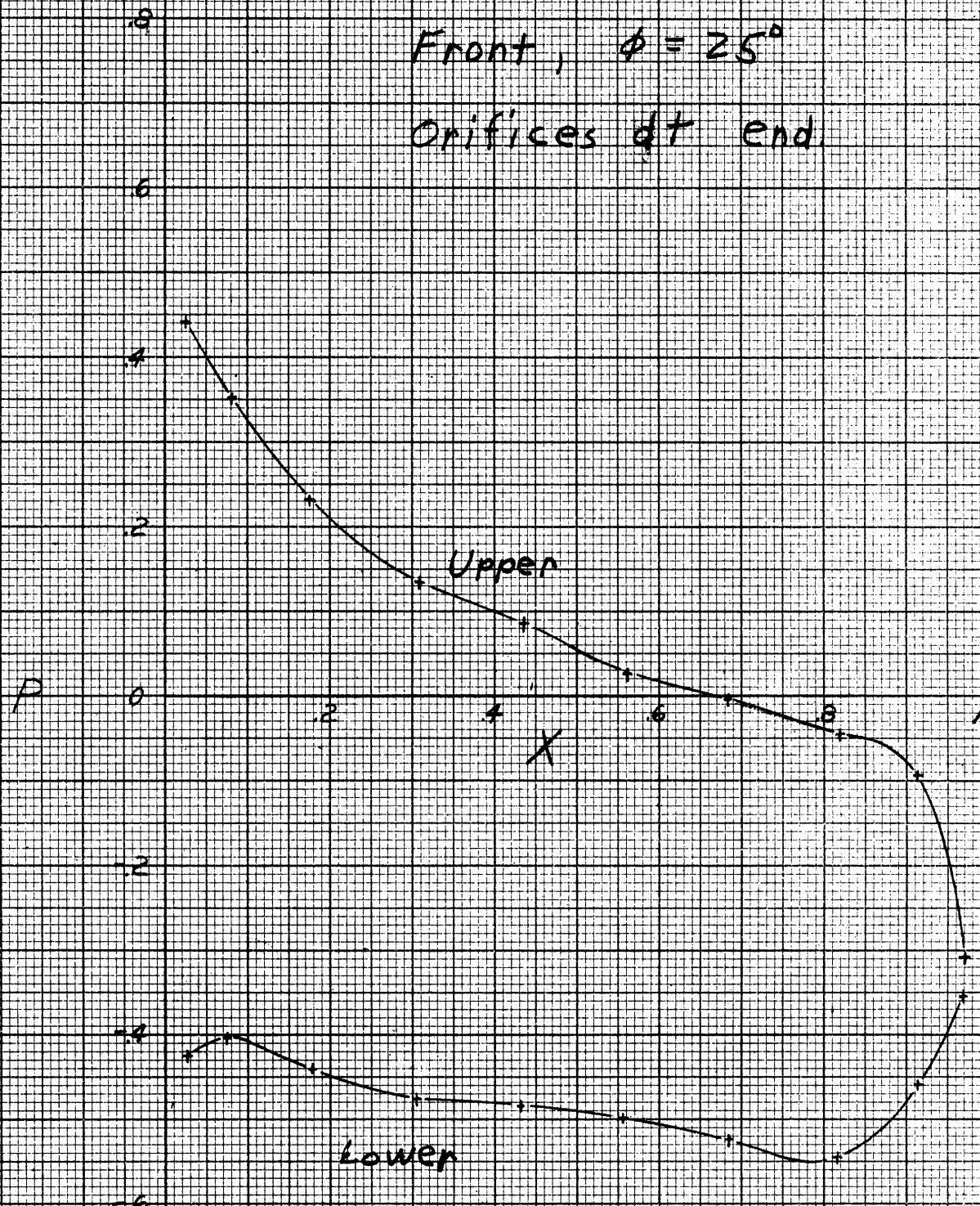

Fig. 17. P vs. X

Rear, $\phi = 25°$

Orifices at end.

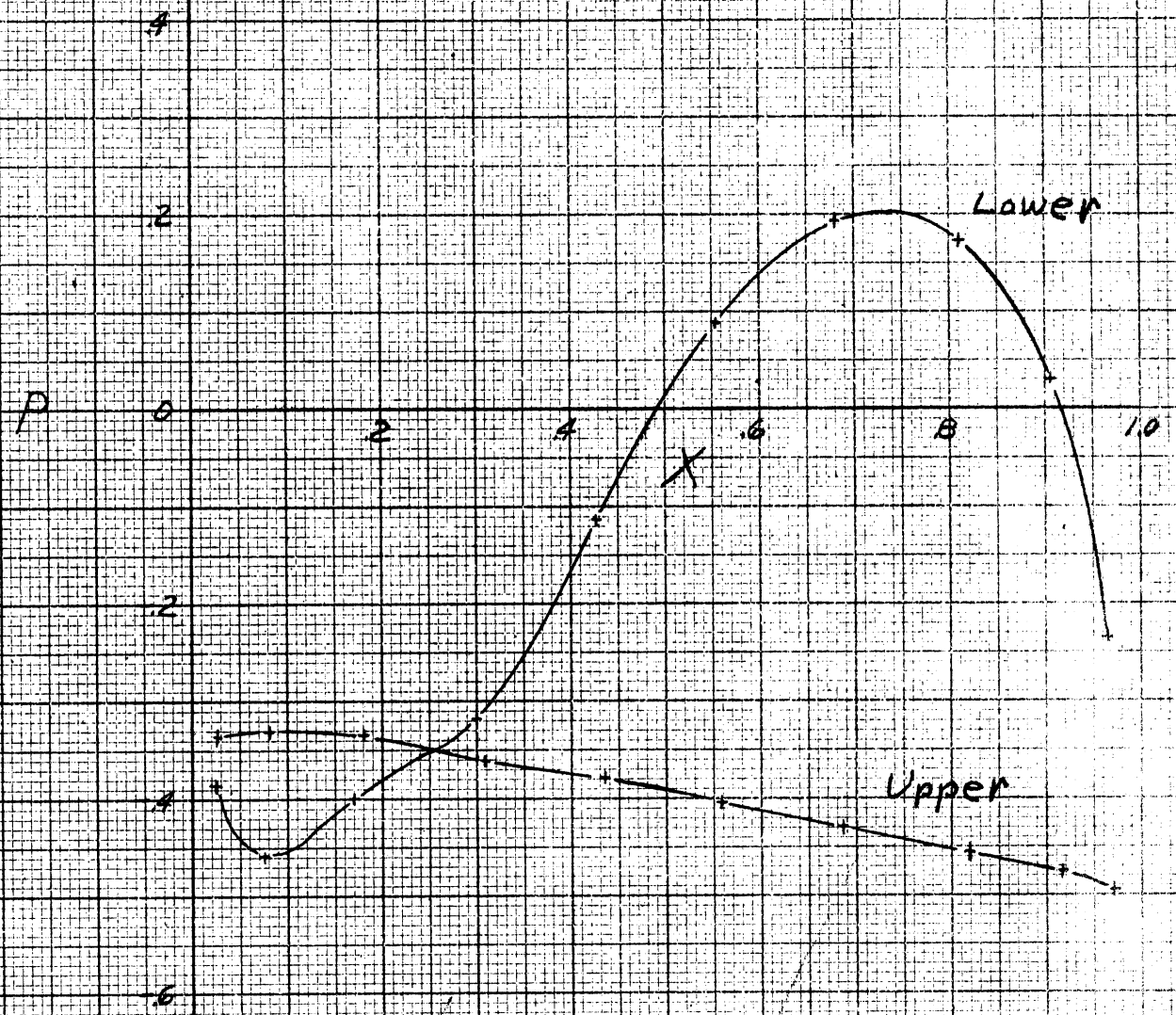

Fig. 18. P vs. X

Front, $\phi = 25°$

Orifices at quarter point.

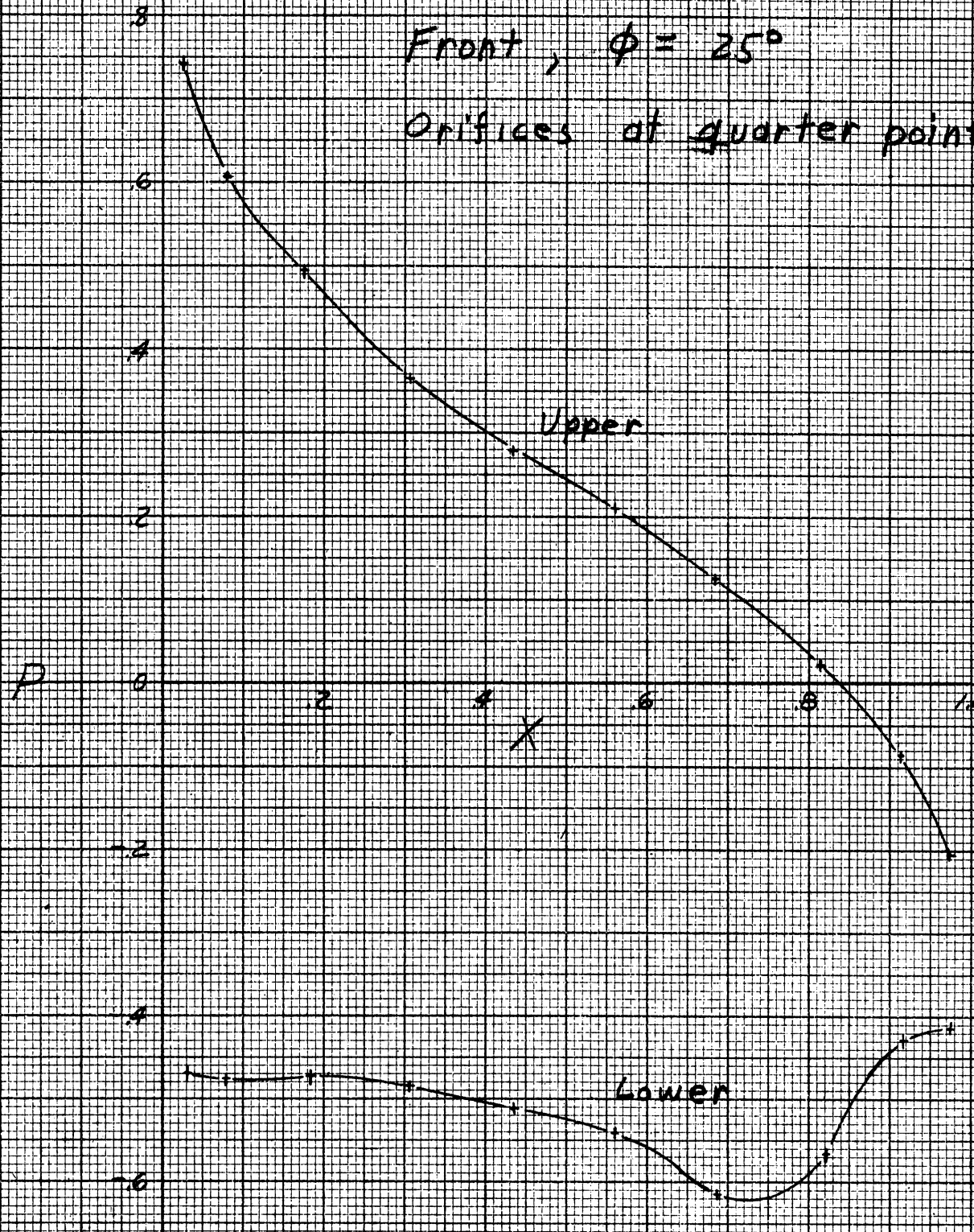

Fig. 19. P vs. X

Rear, $\phi = 25°$

Orifices at quarter point.

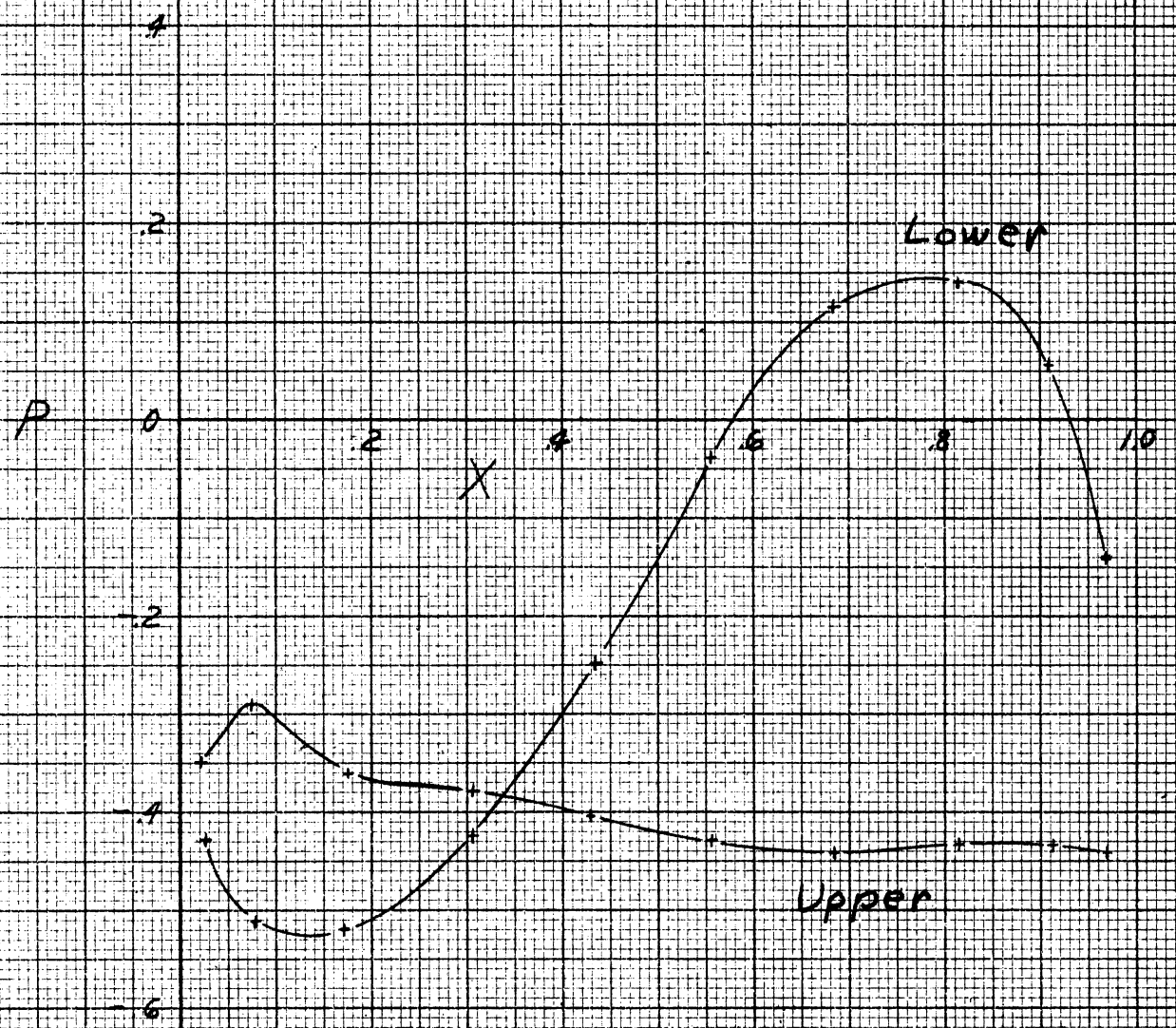

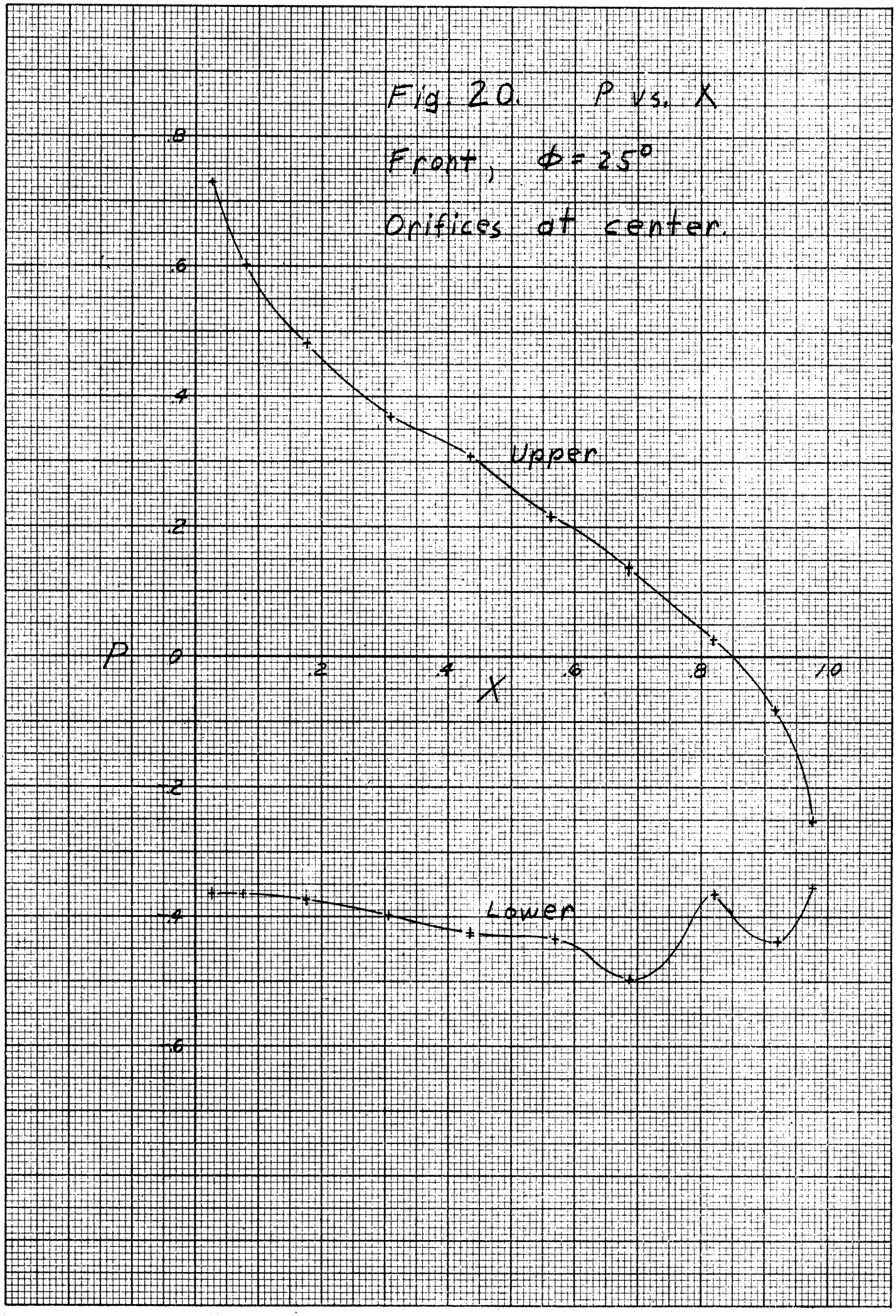
Fig. 20. P vs. X
Front, Φ = 25°
Orifices at center.
.8
.6
.4
.2
0
-.2
-.4
-.6
P
.2
.4
.6
.8
1.0
X
Upper
Lower

Fig. 21. P vs. X

Rear, $\phi = 25°$

Orifices at center.

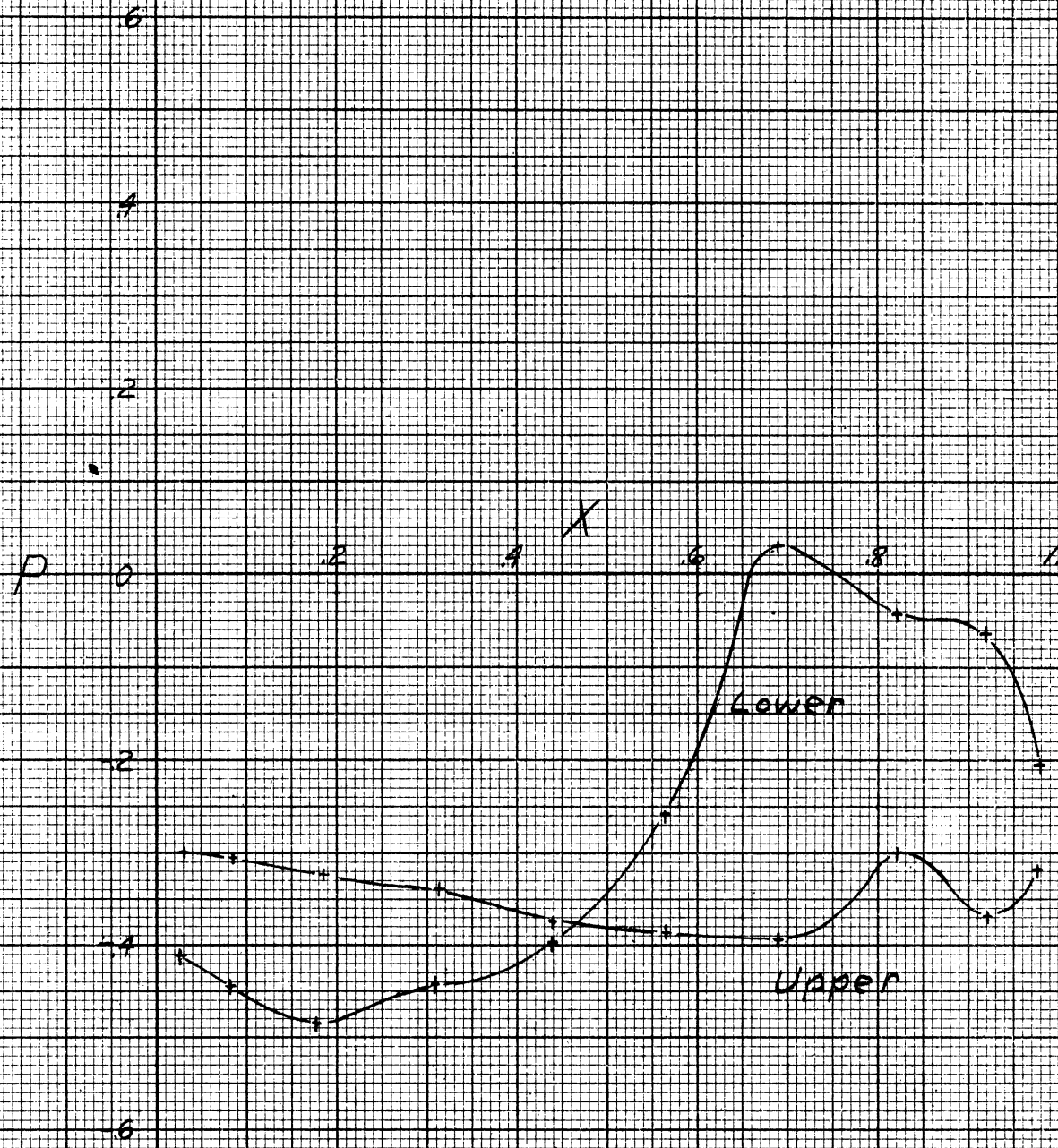

Fig. 22. P vs. X

Front, $\phi = 30°$

Orifices at end

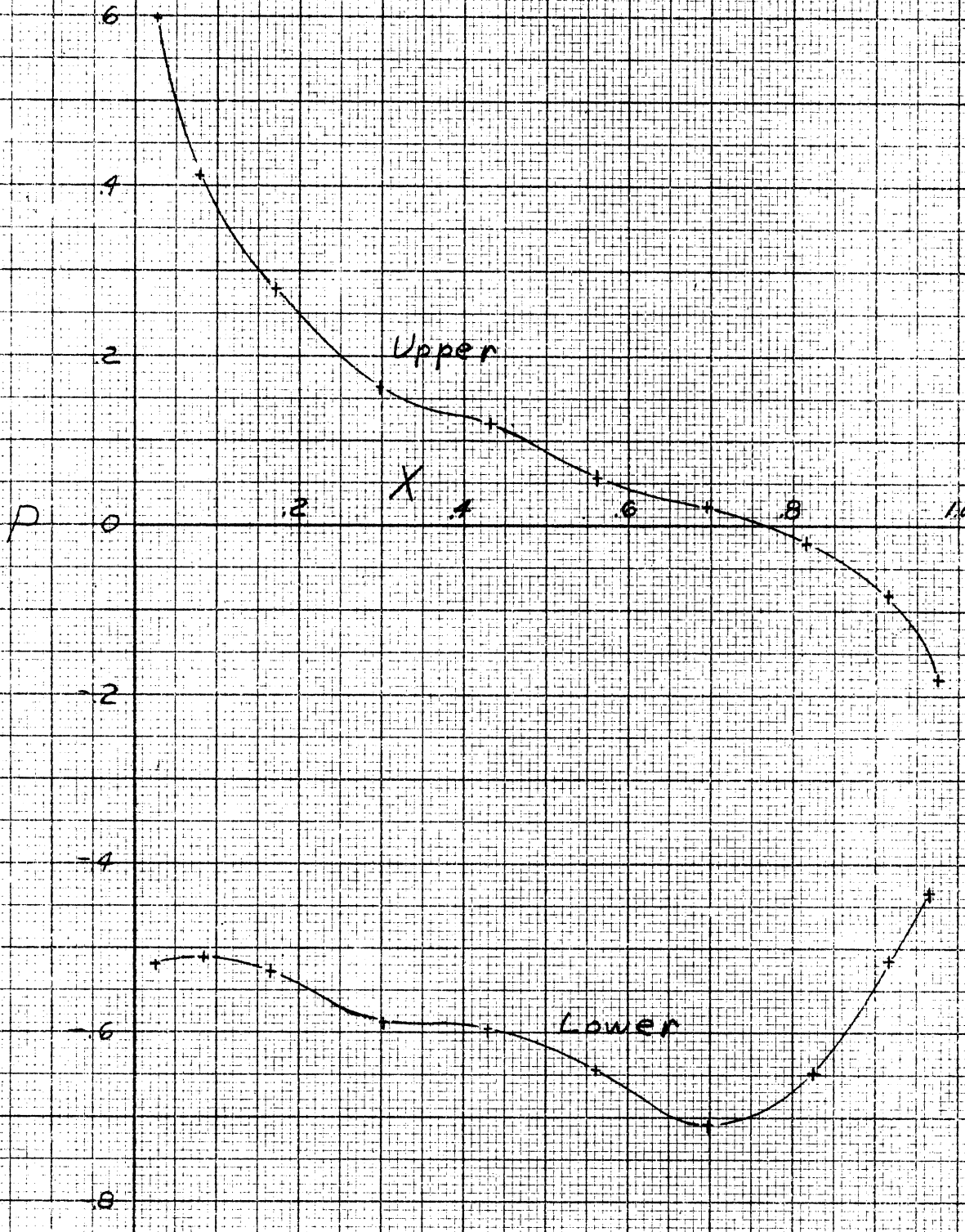

Fig. 23. P vs. X

Rear, $\phi = 30°$

Orifices at end.

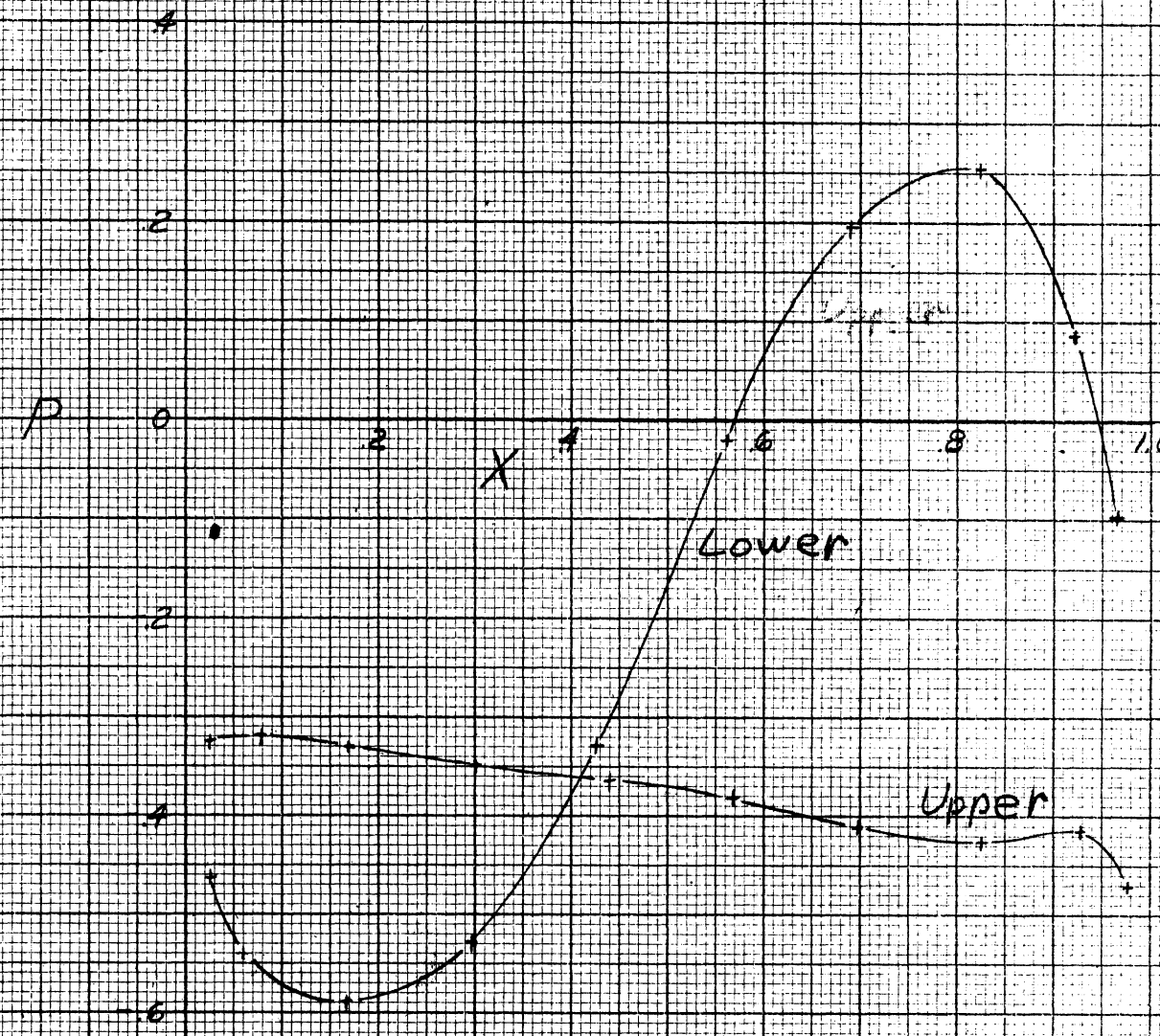

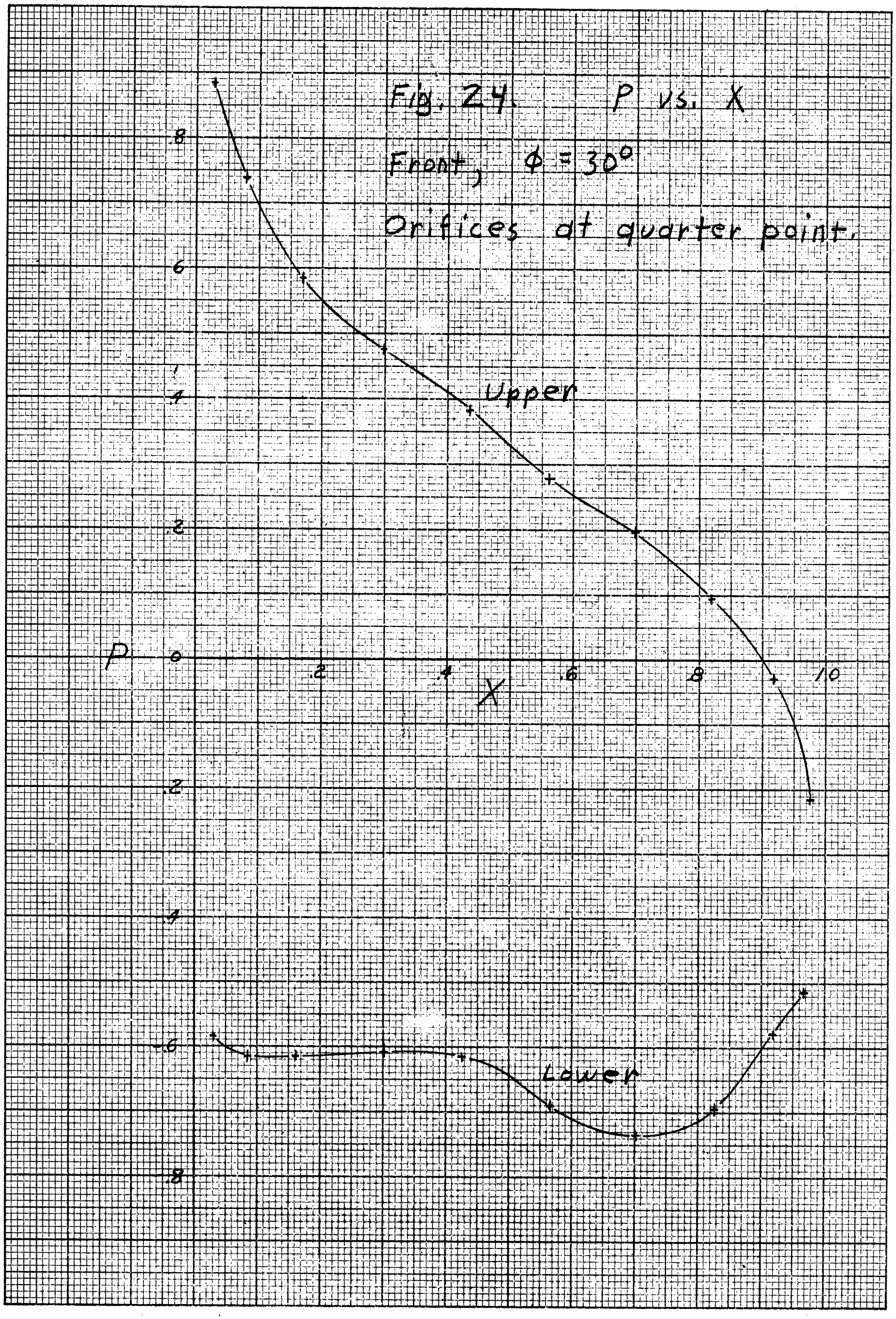
Fig. 24 P vs. X
Front, $\phi = 30°$
Orifices at quarter point.
.8
.6
.4
.2
P
0
.2
.4
X
.6
.8
1.0
Upper
Lower
.2
.4
.6
.8

Fig. 25 P vs. X

Red_r, $\phi = 30°$

Orifices at quarter point.

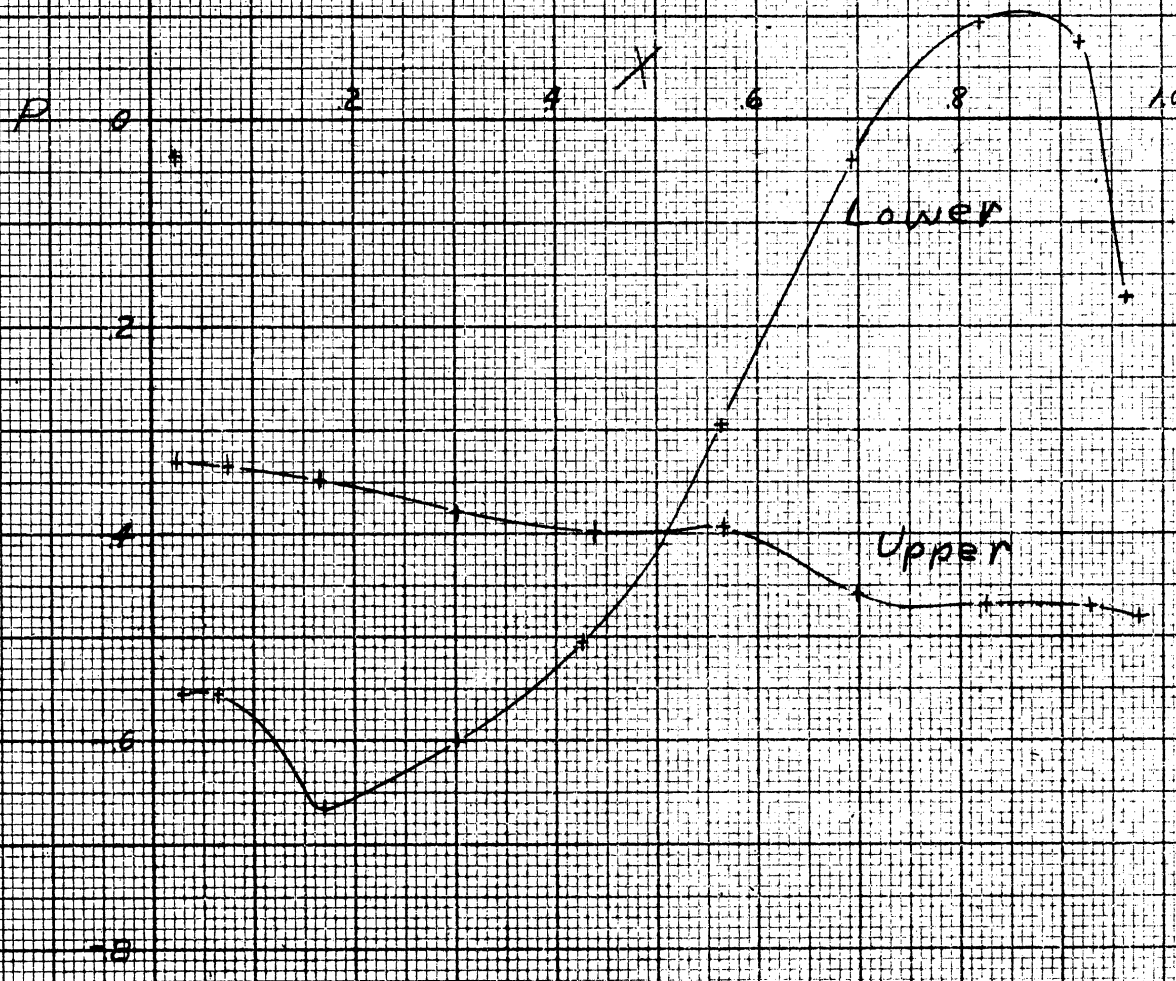

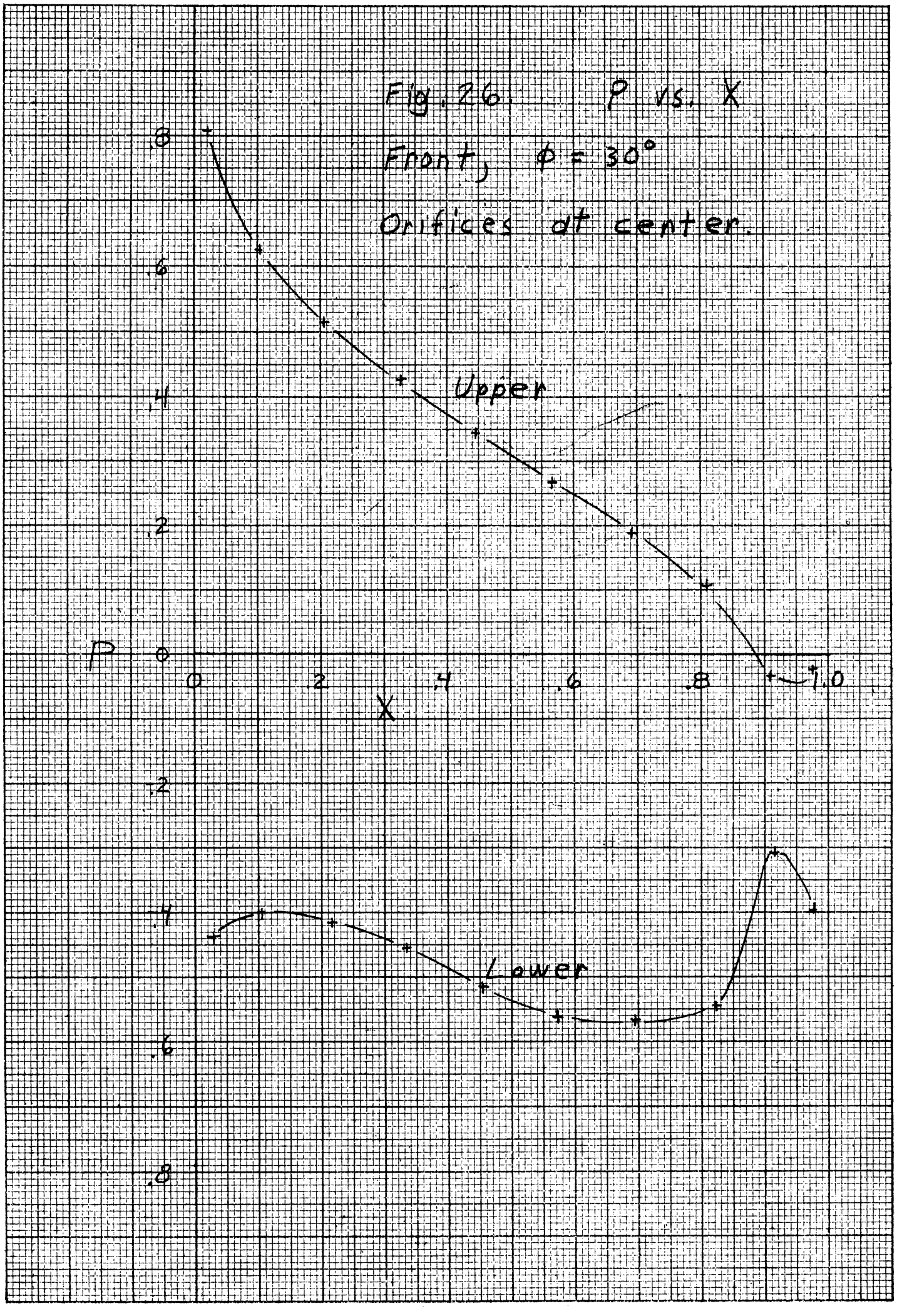
Fig. 26. P vs. X
Front, φ = 30°
Orifices at center.
Upper
Lower
P
X
.8
.6
.4
.2
0
.2
.4
.6
.8
1.0
.2
.4
.6
.8

Fig. 27 P vs. X

Rear, $\phi = 30°$

Orifices at center.

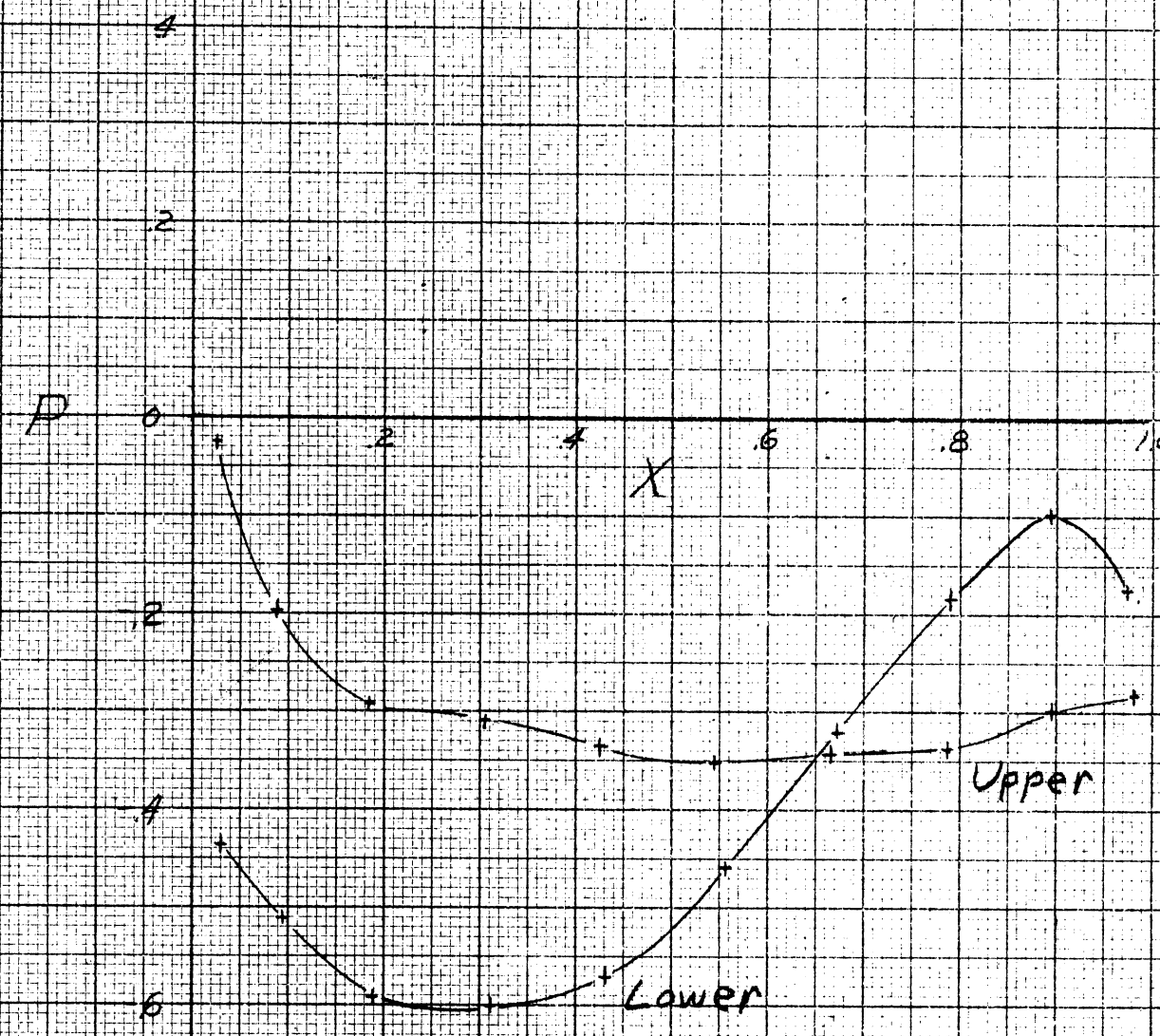

Fig. 28. c_m vs. y.